FEDERAL UNIVERSITY OF PARÁ
INSTITUTE OF EXACT AND NATURAL SCIENCES
GRADUATE PROGRAM IN COMPUTER SCIENCE

PAULO TADEU RESQUE DE SOUZA

A MACHINE LEARNING FRAMEWORK TO DETECT EPILEPTIC SEIZURES AND PRIORITIZE DATA TRANSMISSION IN INTERNET OF MEDICAL THINGS

Belém

2020

PAULO TADEU RESQUE DE SOUZA

A MACHINE LEARNING FRAMEWORK TO DETECT EPILEPTIC SEIZURES AND PRIORITIZE DATA TRANSMISSION IN INTERNET OF MEDICAL THINGS

Doctorate Thesis submitted to the Post-Graduate Computer Science Program in the Natural and Exact Science Institute at Federal University of Pará as required to obtain the Doctorate Degree in Computer Science.

Advisor: Prof. Dr. Denis Lima do Rosário

Co-advisor: Prof. Dr. Eduardo Coelho Cerqueira

Belém

2020

Dados Internacionais de Catalogação na Publicação (CIP)

R429m Resque, Paulo, 2020-

A Machine Learning Framework to detect epileptic seizures and prioritize data transmission in Internet of Medical Things / Paulo Tadeu Resque de Souza. - Belém, 2020.

Advisor: Prof. Dr. Denis Lima do Rosário;
Co-advisor: Prof. Dr. Eduardo Coelho Cerqueira.
Thesis (Doctorate) - Federal University of Pará , Institute of Exact and Natural Sciences, Graduate Program in Computer Science, Belém, 2020.

1. Dispositivos Médicos 2. Aprendizagem de Máquina 3. Comunicação I. Título.

CDD: 004.66

UNIVERSIDADE FEDERAL DO PARÁ
INSTITUTO DE CIÊNCIAS EXATAS E NATURAIS
PROGRAMA DE PÓS-GRADUAÇÃO EM CIÊNCIA DA COMPUTAÇÃO

PAULO TADEU RESQUE DE SOUZA

A MACHINE LEARNING FRAMEWORK TO DETECT EPILEPTIC SEIZURES AND PRIORITIZE DATA TRANSMISSION IN INTERNET OF MEDICAL THINGS

Tese de Doutorado apresentada ao Programa de Pós-Graduação em Ciência da Computação da Universidade Federal do Pará como requisito para obtenção do título de Doutor em Ciência da Computação, defendida e aprovada em 30/11/2020, pela banca examinadora constituída pelos seguintes membros:

Prof. Dr. Denis Lima do Rosário
Orientador – PPGCC/UFPA

Prof. Dr. Eduardo Coelho Cerqueira
Co-orientador – PPGCC/UFPA

Prof. Dr. André Figueira Riker
Membro Externo – FACOMP/UFPA

Prof. Dr. Helder May Nunes da Silva Oliveira
Membro Externo – FACOMP/UFPA

Profa. Dra. Thaís Lira Tavares dos Santos
Membro Externo – UFPA

Visto:
Prof. Dr. Nelson Cruz Sampaio Neto
Coordenador do PPGCC/UFPA

I devote this work to my family for their unconditional love and support throughout my life.

Acknowledgement

I dedicate my sincere thanks to:

–Prof. Dr. Denis Rosário, for the guidance, dedication and effort offered to make this work possible.

–Prof. Dr. Eduardo Cerqueira, for the guidance, encouragement and for the confidence that he placed in me.

–Prof. Drs. Aldri Santos, Michele Nogueira, Cristiano Both and Jéferson Noble, for the hours in meeting in the Hangout and Skype to discuss about this work.

–The professors on the gradute program in computer science for sharing the knowledge who pave the way of many aspects of this research.

–The team members of the GERCOM laboratory especially to the research colleagues Alex, Iago, Lucas, Nagib, Thais, Fabio, Felipe, and Hugo, by the aid in diverse moments.

–The students of UFPR Andressa Vergütz and CESUPA Stefany Pinheiro for the help in the experiments.

–The physicist Benedito Pedro Resque Oliveira, for his advice on epilepsy syndrome, diagnosis and therapy.

–The Prof. Luiz de Oliveira Xavier, for his professional example which encouraged me to engage in a Doctorate program.

This work was supported by the joint NSF and RNP HealthSense project, grant #99/2017 and by the R&D project entitled "IoT-Cloud de Medição de Energia Centralizada Voltado a Rede CEA", process number 001/2017. This work was also financed by FAPESPA ICAAF N 003/2017.

"The BEST for the group comes when everyone in the group does what's best for himself AND the group."
John Nash

Abstract

A Machine Learning Framework to detect epileptic seizures and prioritize data transmission in Internet of Medical Things

Advisor: Prof. Dr. Denis Lima do Rosário
Co-advisor: Prof. Dr. Eduardo Coelho Cerqueira
IoMT Application, Wearable Devices; Machine Learning; Clinical Diagnostic; Data Traffic Prioritization.

New technologies come on stage every day, and the technological advances enhance the user's experience. In this context, wearable devices are an emerging technology that delivers a better user experience in many daily activities. In the healthcare industry, the Internet of Medical Things (IoMT) architecture composed of body sensors, network communication gateways, and central servers relies on wearable devices to sense, collect, and continuously transmit the patient's physiological information supporting the medical crew. In this scenario, chronic patients, such as people with epilepsy, require continuous monitoring outside hospital premises. However, medical diagnosis and treatment for syndromes like epilepsy demand data availability, transmission reliability, low network transmission delay, and fast detection procedure. Thus, an IoMT application for epileptic seizure detection processing the patient's physiological data near the sensor device and transmitting only the diagnostic information fulfill such requirements. In this thesis, we propose an Machine Learning (ML) framework to identify a physiological traffic flow among other transmitted data, proceed with a clinical diagnostic on a communication gateway, and prioritize the data transmission in a Wireless Fidelity (WiFi) network to a hospital cloud server. The solution consisting of two modules for clinical diagnostic and information transmission accomplish promising results during simulations. Our proposal achieve 91.57% accuracy in detecting and assigning a priority tag to a physiological stream, 97.76% accuracy in detecting epileptic seizures from Electroencephalography (EEG) signal, and 60% improvement in Packet Delivery Rate (PDR) for physiological data transmission in a WiFi.

Contents

List of Abbreviations

ABP Arterial Blood Pressure

AC Access Category

AIRS Artificial Immune Recognition System

AIFSN Arbitration Inter-Frame Space Number

ANFIS Adaptive Neuro-Fuzzy Inference System

ANN Artificial Neural Networks

AP Access Point

AQCA Adaptive Quality of Service Computational Algorithm

AuC Area under the ROC Curve

BLE Bluetooth Low Energy

CART Classification and Regression Tree

CCN Content-Centric Network

CHAID Chi-squared Automatic Interaction Detector

CSV comma-separated values

CSMA/CA Carrier Sense Multiple Access/Collision Avoidance

CVP Central Venous Pressure

CW Contention Window

DCF Distributed Coordination Function

DFT Discrete Fourier Transform

DT Decision Tree

ECG Electrocardiography

EC-GSM Extended Coverage Global System for Mobile Communication

EDCA Enhanced Distributed Channel Access

EEG Electroencephalography

EMG Electromyography

FFT Fast Fourier Transform

FT Fourier Transform

FP/h false positives per hour

HCCA HCF controlled channel access

HCF Hybrid Coordination Function

HR Heart Rate

HRI Heart Rate Increase

HRV Heart Rate Variability

ICU Intensive Care Unit

I-ICA Infinite Independent Component Analysis

iEEG Intra-Cranial EEG

IoT Internet of Things

IoMT Internet of Medical Things

ID3 Iterative Dichotomiser 3

KNN K-Nearest Neighbor

KPI Key Performance Indicators

LPWAN Low Power Wide Area Network

LTE Long Term Evolution

LTE-M Long Term Evolution for Machines

MAC Medium Access Control

MCCA MCF Controlled Access

MGH-MF The Massachusetts General Hospital-Marquette Foundation

ML Machine Learning

MLP Multi Layer Perceptron

NB Naïve Bayes

NB-IoT Narrow Band Internet of Things

NFC Near Field Communication

PAP Pulmonary Artery Pressure

PCA Principal Component Analysis

PCF Point Coodination Function

PDR Packet Delivery Rate

PPG Photoplethymography

PPV positive prediction value

PRV Pulse Rate Variability

PSNR Packet Signal-to-Noise Ratio

QoE Quality of Experience

QoS Quality of Service

RF Random Forest

RNN Recurrent Neural Network

ROC Receiver Operating Characteristics

STA Station

SVM Support Vector Machine

TXOP Transmission Opportunity

UCI University of California at Irvine

WiFi Wireless Fidelity

WHO World Health Organization

WT Wavelet Transform

WBAN Wireless Body Area Network

WWBAN Wearable Wireless Body Area Network

List of Figures

List of Tables

CHAPTER 1

Introduction

The increasing adoption of mobile technologies enhances the user‘s experience in many fields. In this scenario, the use of wearable technologies presents consistent growth year over year. The introduction of wearable technologies in the healthcare industries opens new frontiers for better therapy follow up in the IoMT frame. Koutras *et al.* [1] defines IoMT as the association of Internet of Things (IoT) technologies with healthcare services for remote patient monitoring. The IoMT refers to a set of sensor devices, communication gateways, and service application cooperating to provide better user‘s experience during clinical diagnosis and treatment. In this work, the application scenario considers the monitoring of chronic patients outside hospital premises, where physiological data transmission competes for medium access with several traffic types. This chapter introduces the concepts behind the project, in the context of IoMT applicability in the healthcare industry.

1.1 Overview

According to a recent report, Ericsson forecasts up to 25 billions connected IoT devices by 2025 [2]. In this context, the report classifies the IoT devices as Massive, Broadband, and Critical [3]. Specifically, massive IoT refers to applications that require a large number of IoT devices spread in a wide area network. On the other hand, broadband IoT relates to usage cases requiring throughput higher than Massive IoT. Finally, the fundamental aspects of Critical IoT relay on low latency and ultra-high reliability networks [2]. Hence, these different classification implies in distinct network and device's requirements in terms of coverage area, energy efficiency, communication reliability, data throughput, network latency, and implementation cost.

The technological advance already provides individuals with personalized IoT de-

vices. Seneviratne *et al.* [4] describes wearable devices as personal mobile devices in the form of accessories, textiles, and patches, capable of delivering solutions that smartphones alone cannot handle. The products depicted in Figure 1 are some current examples of wearable devices applicable to different sectors. The increasing number of options leads to the belief that individuals will wear multiple devices simultaneously in both professional and non-professional applications. On the one hand, professional devices require sensing accuracy, better security schemes, low-energy consumption, low network latency, and fault-tolerant networks. On the other hand, non-professional appliances aimed for personal amusement do not share the same application requirements as professional usage cases.

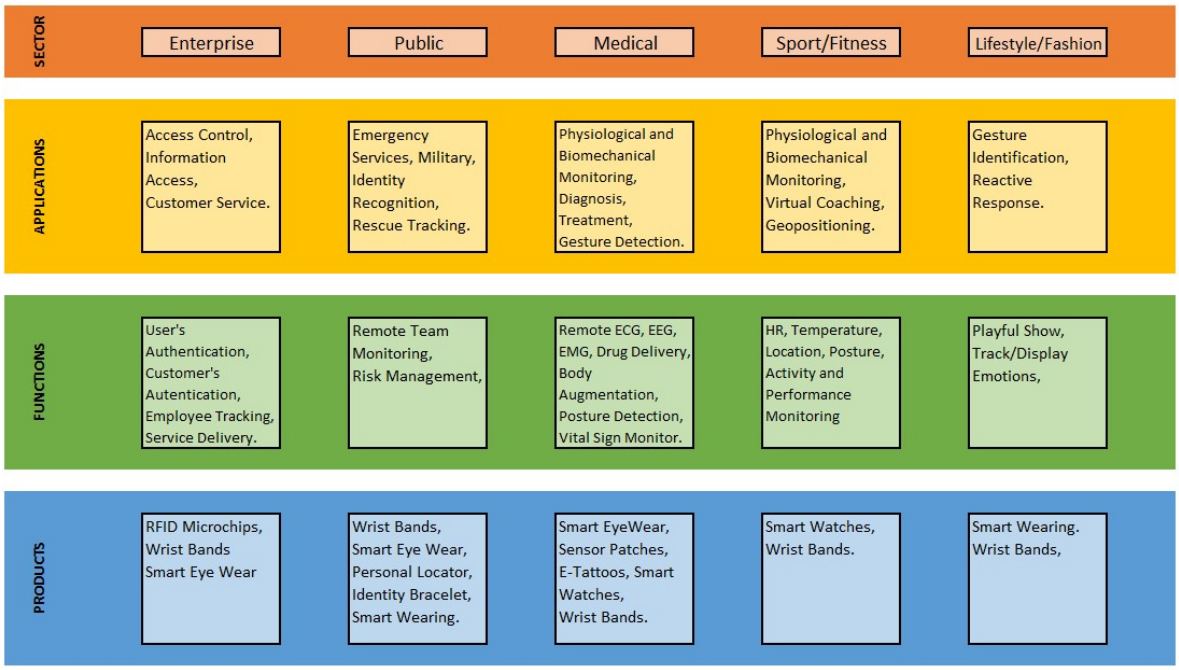

Figure 1: Wearables products, functions, and applications per sector

These new technologies drive the healthcare industry to a higher level of medical assistance, offering better therapy and life quality for patients. In this context, older adults with chronic conditions require continuous monitoring for prolonged periods. However, monitoring patients in hospitals and clinics presses for resources in the healthcare industry. Thus, IoT devices became an alternative for monitoring patients for more prolonged periods outside hospital premises. In this way, the IoMT consisting of professional applications, services, and platforms for telemedicine attracts the research attention from the healthcare industry [5, 6, 7, 8]. Hence, IoMT relies on wearable devices to continuously sense, collect, and transmit biometry data, leveraging for an onboard radio wireless facility to communicate with a gateway, which in turn delivers the collected data across the internet to an e-Health system [9, 10, 11].

1.2 Motivation and Challenges

Older adults with chronic conditions, such as diabetes, cardiovascular diseases, and epilepsy, requiring continuous monitoring rely on IoMT to improve the Quality of Service (QoS) within healthcare assistance. In this context, wearable devices consisting of IoMT appliances to collect vital signs implement a choice of short-range wireless technology to transmit the information [10, 11]. Typically, the transmission using short-range communication technologies such as Bluetooth Low Energy (BLE), Near Field Communication (NFC), and WiFi are prone to several interference sources. The coexistence of technologies sharing the same frequency spectrum [12] and collisions [13], are examples of interference sources during transmission. These interference sources reduce the QoS perceived within the IoMT application. Thus, processing the vital sign information near the sensor devices, *e.g.*, in the communication gateway is an alternative to bypass some of the interference sources and address the near-real-time requirement for IoMT applications [14, 15, 16].

Typically, a time series with samples of the monitored vital sign represents the individual's physiological information. The continuity nature of physiological data collection drives the requirement for continuous analysis. In this context, the introduction of an automatic analytical technique is paramount for the application QoS. Hence, ML constitute a promising technique for pattern recognition, and clinical diagnostic [17, 18, 19]. Additionally, the application of an ensemble classifier potentially enhances the ML performance [20]. Moreover, executing the pattern recognition and diagnostic in the communication gateway minimizes the data transmission to the cloud server [10] and the risk of data leakage [5].

The physiological information exhibits diverse characteristics. In this sense, the IoMT devices collect the respective vital sign using different methods, sensor placement, and collection frequency. The differences implicate in differentiated volumes of data to process and transmit. Moreover, each vital sign has relative importance for the clinical diagnostic. Heart Rate (HR) monitoring is predominant for a patient with a cardiological condition, while pulmonary pressure would be more critical if the patient has a lung condition. Hence, each physiological information requires a distinguished processing and transmission QoS [21, 22], depending on the patient's condition.

The strict QoS requirement ensures accurate information for the medical staff. [21, 22]. Nevertheless, wearable medical devices transfer the collected information through a shared wireless network infrastructure [10, 17, 23]. In this sense, the transmission of physiological data for healthcare applications should prevail over regular internet traffic. Thus, it is essential to classify (in a non-intrusive manner) the diverse healthcare traffic flows transmitted from wearable devices in a shared wireless infrastructure [21].

1.3 Research Questions

a. How to use an ML model to address clinical diagnostic and priority transmission in an IoMT scenario with multiple competing applications and traffic characteristics?

b. What are the ML algorithms with less computational complexity and good accuracy for a specific clinical diagnostic, *e.g.*, epilepsy seizure detection?

c. How to provide better QoS in terms of accuracy in detecting epileptic seizures and lower latency in transmitting the diagnostic information to the hospital crew in an IoMT application scenario?

1.4 Objectives

In this thesis, we propose an ML framework to identify the physiological traffic pattern, proceed with the clinical diagnostic based on the vital sign, and prioritize the data transmission to hospital cloud servers in an IoMT application scenario. Addressing these issues would push IoMT applications to a higher level of user experience. Additionally, our proposal minimizes data interception risk as it reduces data exposure in wireless medium access. This research work addresses the following objectives:

- Analyze the ML techniques embeddable in IoMT architecture for use in healthcare solutions.
- Identify applicable ML algorithms for diagnostic procedures, *e.g.*, epileptic seizure detection, from an communication gateway perspective.
- Identify the traffic generated by IoMT medical devices, use the physiological information for clinical diagnostic, and prioritize the diagnostic data transmission to the hospital servers in a scenario of competing for network medium access.

1.5 Text Organization

We present the contributions to this work based on three achievements. First, we present the results of our analysis involving the ML techniques to detect epileptic seizures. Second, we present our strategy to prioritize the transmission of the diagnostic results, based on the scenario of devices and applications competing for medium access in the WiFi network. Finally, we configure the two individual solutions together in the same framework. The remaining of this document is structured as follow:

- Chapter 2: Introduces the theoretical references explored in this work.
- Chapter 3: Presents and analyses the related works.

- Chapter 4: Analyses the ML methods applied to epileptic seizure detection.
- Chapter 5: Defines a method to prioritize medical information transmission on a wireless channel.
- Chapter 6: Concludes this work and defines future research directions.

CHAPTER 2

Basic Concepts

2.1 Epilepsy

Epilepsy is a brain syndrome with different disturbing causes characterized by a non-provoked predisposition to recurrent seizures. It affects the human neurobiological and cognitive functions with psychological and social consequences. According to the World Health Organization (WHO), epilepsy affects from 0.4% to 1% of the global population, and about 70% of patients respond well to treatment [24, 25]. When an individual suffers the first seizure, it is highly probable that a recurrence follows within two years - 40% to 50% chance [26]. Thus, patients who manifested a non-provoked seizure require monitoring for epilepsy confirmation and classification.

During the diagnostic procedures, the EEG is the leading medical test to conclude if the patient has epilepsy [26]. In this context, ambulatory and video EEG are examples of non-invasive methods to register brain activity. The ambulatory EEG consists of a set of electrodes fixed on the patient's scalp at predefined positions [27]. Specifically, the electrodes placement follow the 10-20, 10-10, or 10-5 international system as illustrate in Figure 2 [28]. Alternatively, the intracranial EEG provides an invasive method that adds value to the diagnostic procedure in patients with surgery indication [26]. Signal amplifiers and computer software register the brain's activity as a temporal series of the potential difference between each pair of electrodes. During diagnostic procedures, the medical crew conducts a complete anamnesis and physical examination to conclude for a therapy [29]. The findings during diagnostic procedures update the patient's electronic medical record.

Qaraqe *et al.* [27] describe that relevant brain activity for clinical analysis lies in the range from 0.5 to 50 Hz and seizure activity is within the range from 0.5 to 25 Hz. The brain activity waveform has a δ component when the dominant frequency is

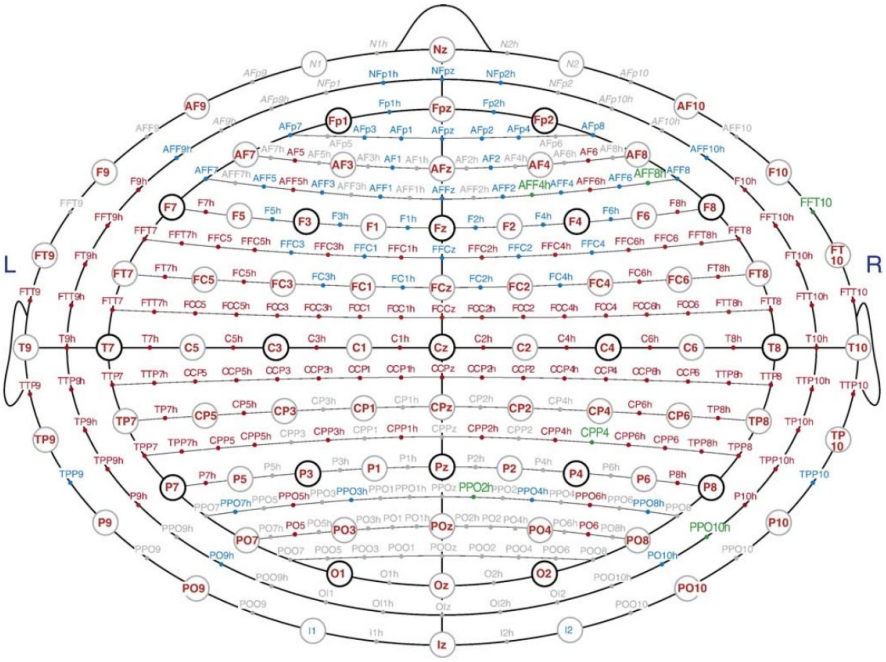

Figure 2: EEG electrodes placement. Black circles indicate 10-20 electrodes placement; gray circles indicate the additional 10-10 electrodes placement; red, blue, and green positions represent the placement where neighbor points can not overlap; the gray positions represents the additional 10-5 electrodes that interfere with neighbor positions. Jurcak *et al.* [28]

$f < 4Hz$, a θ component with $4 < f < 8Hz$, an α component with $8 \leq f \leq 12HZ$, a β with $12 \leq f \leq 30Hz$, and a γ with $f \geq 30Hz$ [27]. The dominant frequency is the one which carries the highest energy within the spectrum [30]. Figure 3 exhibits a typical EEG segment noted from a healthy individual according to the analysis from an expert. A biochemical process initiated at cell level leads to an abnormal brain activity that triggers epileptic seizures [26]. Figure 4 exhibits the abnormal brain behavior, noted from an epileptic patient after expert's analysis. The spike-and-wave characteristics depicted between 40 msec and 70 msec in Figure 4 associates the seizure activity with genetic-origin epilepsy [26].

2.2 Communication Technologies

Alam *et al.* [11] explains that communication is a key issue in the IoT context. The combination of short-range technologies, *e.g.*, NFC, BLE, WiFi, and ZigBee, with long-range, *e.g.*, LoRa, Sigfox, 4G, and NB-IoT, can achieve both efficiency and cost-effectiveness depending on the IoT application scenario. Baker *et al.* [31] discuss communication technologies in the context of healthcare applications. Specifically, the survey explores the frequency band, data rate, coverage range, and the power consumption for each technology. The investigated technologies includes operation in both licensed and unlicensed spectrum, *i.e.*, either require or not a previous negotiation with authorities

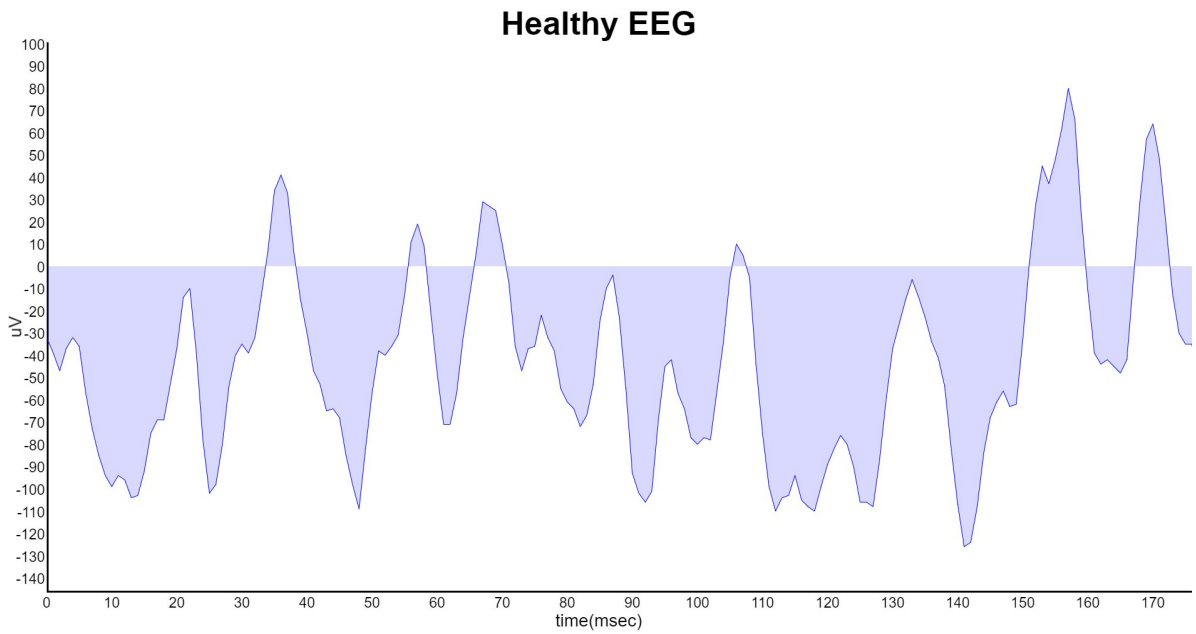

Figure 3: EEG from a healthy individual.

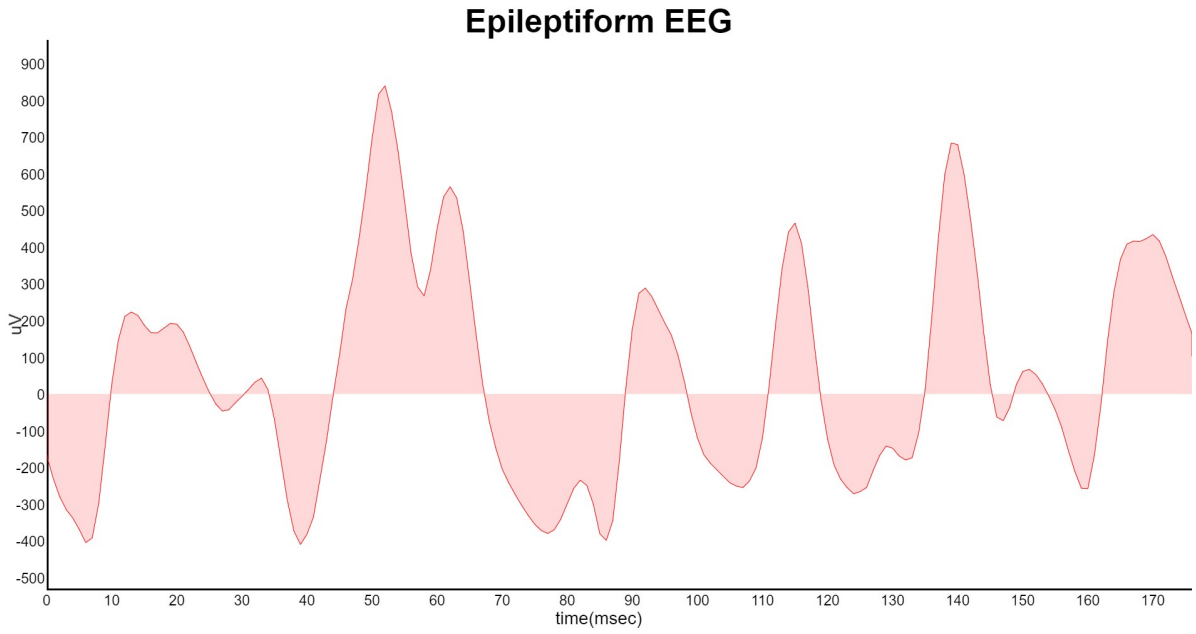

Figure 4: Spike-and-wave aspect (from $40msec \leq time \leq 70msec$) of an EEG during the seizure period.

Table 1: Comparison of short-range and long-range communication technologies, adapted from Ahad *et al.* [34]

	Technology	Frequency	Spectrum	Data Rate	Coverage	Power Usage
Short- Range	NFC	13.56 MHz	Unlicensed	100-400 kbps	10 cm	Very Low
	BLE	2.4 GHz	Unlicensed	1 Mbps	0.1 Km	Low
	Wi-Fi	2.4 GHZ and 5 GHz	Unlicensed	54 Mbps - 1 Gbps	50 m	Low-High
	ZigBee	2.4 GHz	Unlicensed	250 kbps	10-100m	Very Low
Long-Range	LoRa	433/868/915 MHz	Unlicensed	50 kbps	25 Km	Low
	Sigfox	868/915 MHz	Unlicensed	300 bps	50 Km	Low
	4G	800, 1800, 2600 MHz	Licensed	12 Mbps	10 Km	High
	NB-IoT	900 MHz	Licensed	250 kpbs	35 Km	High

for the right to access a frequency band.

It is notable in Table 1 that technologies sharing the spectrum may interfere with each other. Technologies transmitting in the unlicensed spectrum with low or very low energy consumption offer few possibilities to provide QoS for critical IoMT devices. For instance, LoRa technology implements a pure ALOHA-based medium access protocol [32]. Thus, LoRa is not indicated for critical applications requiring real-time data transmission [33]. Moreover, Kim *et al.* [12] discusses the coexisting problems involving ZigBee and WiFi. Specifically, the authors emphasize the interference aspect in the coincident channels, which increases the collisions and reduces the QoS. In this scenario, Kim *et al.* [12] propose an algorithm to control the traffic load in the WiFi network. In an IoMT context, where a chronic patient require monitoring outside hospital premises, *e.g.*, a home care facility, the WiFi technology offer good balance between coverage, power usage, and data rate to transmit physiological information.

2.3 IEEE 802.11

The IEEE 802.11 set of amendments define the standard for wireless communication in a local area network, specifying the network medium access control and physical layers [35]. The standard allows devices to operate in any compatible network, providing authentication methods, dynamic frequency selection, QoS mechanism, operating in the presence of coverage overlapping, and more. The standard defines two MAC architectures, respectively, for non-directional and directional multi-gigabit Station (STA). In this work, we focus on non-directional multi-gigabit STA and follow the MAC architecture exhibit in Figure 5 extracted from the IEEE standard [35].

The primary access methodology implemented in this architecture is the Carrier Sense Multiple Access/Collision Avoidance (CSMA/CA). In this methodology, the STA sense the medium before trying to transmit. If the channel is idle, then the STA starts transmitting; otherwise, it will remain on hold expecting the current transmission to finish. After each successful transmission, the STA backs off for a random period before trying to transmit again. The 802.11 standard combines contention-based and contention-free methodologies to provide QoS for the STA. In the newest amendments such as 802.11ah,

the Enhanced Distributed Channel Access (EDCA), which is a contention-based method, became the most adopted implementation.

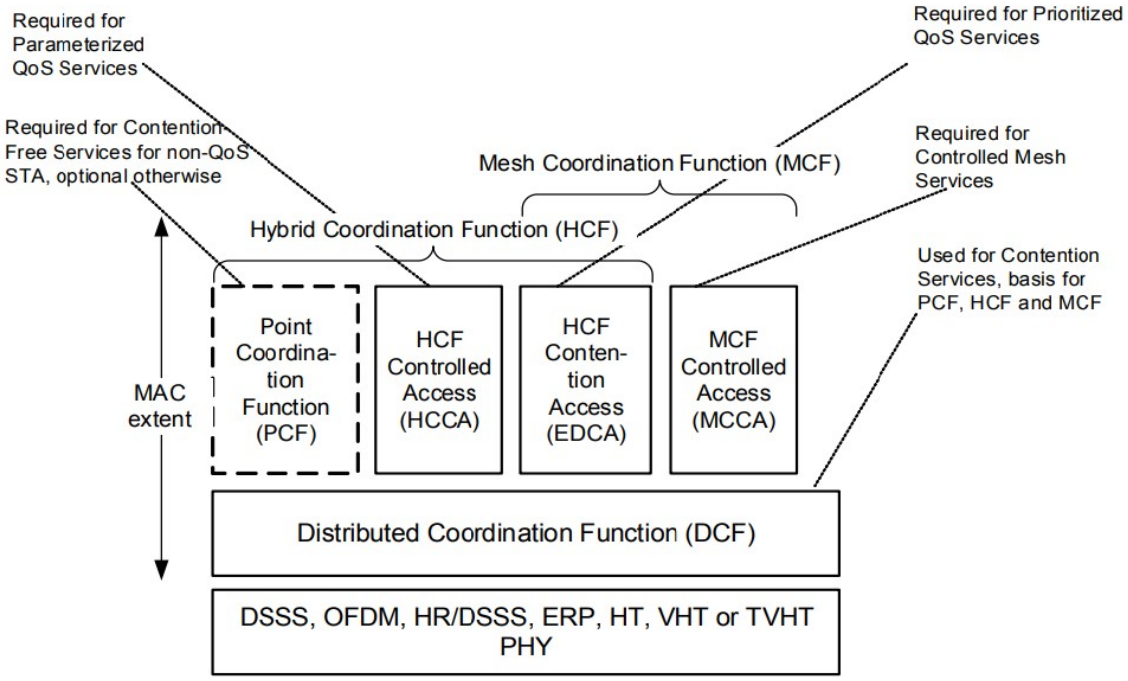

Figure 5: Non-directional multi-gigabit stations MAC architecture. [35]

The EDCA method implements eight user priorities distributed in four Access Category (AC) queues, combining three parameters: the Contention Window (CW), the Arbitration Inter-Frame Space Number (AIFSN), and the Transmission Opportunity (TXOP) [35]. The Access Point (AP) announces these parameters for the STA. The CW is the random time interval that an STA waits before starts transmitting when identifies the channel as idle. The CWmin and CWmax respectively refer to the minimum and maximum values for the CW. The AIFSN defines the time interval between two consecutive transmissions from the same STA. The AP keeps this value lower to increase the successful transmission probability for delay-sensitive STA. The TXOP scheme allows the STA to transmit multiple frames after granting medium access, given the condition of not exceeding the TXOP limit [36]. The summary of possible parameters in the EDCA implementation is an exhibit in Table 2.

Table 2: EDCA Parameters in 802.11 standard. [35]

Priority	User Priority	AC	Transmit Queue (do122Alternate-EDCAActivated false or not present)	Transmit Queue (dot11AlternateEDCAActivated true)	Designation	CWmin	CWmax	AIFSN	TXOP limit
Lowest	1	AC_BK	BK	BK	Backgroud	aCWmin	aCWmax	7	0
	2	AC_BK	BK	BK	Backgroud				
	0	AC_BE	BE	BE	Best Effort	aCWmin	aCWmax	3	0
	3	AC_BE	BE	BE	Best Effort				
	4	AC_VI	VI	A_VI	Video (alternate)	(aCWmin+1)/2-1	ACWmin	2	0
	5	AC_VI	VI	VI	Video (primary)				
	6	AC_VO	VO	VO	Voice (primary)	(aCWmin+1)/4-1	(aCWmin+1)/2-1	2	0
Highest	7	AC_VO	VO	A_VO	Voice (alternate)				

2.4 Chapter Conclusion

The concepts explored in this chapter helps the understanding of the problems we address in this work. Epilepsy affects a significant number of individuals, in the order of 1% of the world population. Explaining the brain syndrome dynamics and the clinical diagnosis procedure helps to understand the importance of accurate and convenient methods to follow up on the therapy. When it comes to communication, many technologies propose a solution in the context of IoT or IoMT. However, only a few technologies provide features to enhance the QoS for delay-sensitive applications. In this scenario, WiFi is popular and affordable in many use-cases outside hospital premises. The next chapters explore these background concepts to come-up-with an integrated solution to detect epileptic seizures and transmit the relevant information with higher priority in a shared WiFi network.

CHAPTER 3

Related Works

This Chapter introduces the works related to this research project highlighting the state-of-the-art and open issues. In Section 3.1, we explore the general application of ML for epilepsy detection. Specifically, we analyze the ML algorithms trained to detect epileptic seizures from physiological signals such as EEG, Electrocardiography (ECG), and Photoplethymography (PPG). Moreover, the related works combine different physiological features in the time domain, frequency domain, or hybrid approaches. In Section 3.2, we discuss the context of patient monitoring outside hospital premises. In this scenario, a medical device from the IoMT application competes for medium access in the wireless network with a generic STA. We then analyze the methods and techniques defined in the wireless network standards in the context of proposed improvements for the medium access control. The two sections aim to establish a baseline for our proposition.

3.1 Epilepsy Detection using Machine Learning

Many of the researches discuss in this section base the investigation on the dataset collected initially by Andrzejak *et al.* [37]. Investigating the dynamic characteristics of brain activity, Andrzejak *et al.* recorded the EEG time series from healthy individuals and epileptic patients. The recording from healthy patients considered the ambulatory EEG obtained from the scalp, with electrodes placement following the 10-20 international system (see Figure 2). The authors noted that healthy volunteers were relaxed and awake during EEG recording. Recording from epileptic patients considered intracranial electrodes, implanted in patients with surgical indication. The intracranial electrodes placement considered the Intra-Cranial EEG (iEEG) collection from a tumor region and its opposite (healthy) brain hemisphere. In such a scheme results in five different EEG time series: *(i)* Healthy patients recorded with their eyes closed; *(ii)* Healthy patients recorded

with their eyes open; *(iii)* Epileptic patients recorded from the epileptic zone during a seizure; *(iv)* Epileptic patients recorded from the epileptic zone during a seizure-free period; *(v)* Epileptic patients recorded from the healthy brain zone (opposite hemisphere from epileptic zone).

Güler *et al.* [38] analyze the EEG dataset [37] and classify epileptic seizures using Recurrent Neural Network (RNN) with Lyapunov exponents trained with Levenberg-Marquardt algorithm. Lyapunov exponents are quantitative measures used in many biological nonlinear systems to characterize its dynamical properties. Biological nonlinear systems include heartbeats dynamics [39] and also brain activity behavior [37]. Güler *et al.* [38] considers three EEG time series out of the five available in the Andrzejak *et al.* dataset. Specifically, the subsets include healthy individuals with their eyes open, epileptic patients recorded during a seizure-free interval, and epileptic patients recorded during a seizure.

Güler *et al.* [38] analysis consider a rectangular window consisting of 256 discrete data points for each EEG signal. Following the investigation, the study calculates the Lyapunov exponents from the recognized sign within the window. The study reduces the dimensionality of the Lyapunov exponents selecting four statistical measurements: *(i)* Mean of the absolute values of the Lyapunov exponents; *(ii)* Maximum of the absolute values of the Lyapunov exponents; *(iii)* Average power of the Lyapunov exponents; *(iv)* Standard Deviation of the Lyapunov exponents.

The proposal applies these four statistical features to train the RNN and achieves 96.79% of positive epilepsy classification. However, the calculation of the Lyapunov exponents is time-consuming, and noise in the time series has adverse effects in the exponent's estimations [40]. Finally, the computational cost of training the RNN using the Levenberg-Marquardt algorithm is $O(n^3)$, where n is the number of neurons in the hidden layer of the RNN. The asymptotical complexity can be reduced to $O(n^2)$ using parallel processing, such as presented by Bilski *et al.* [41].

Güler and Übeyli [42] propose the use of Wavelet Transform (WT) for feature extraction and Adaptive Neuro-Fuzzy Inference System (ANFIS) for epilepsy classification. WT is a variation of Fourier Transform (FT) to analyze signal frequency components with the advantage of removing the noise while preserving features. ANFIS combines the characteristics of both Artificial Neural Networks (ANN) and Fuzzy systems. Specifically, ANFIS uses ANN to determine fuzzy sets and rules.

The analysis in Güler and Übeyli [42] considers all five EEG time series available after Andrzejak *et al.* [37]. The application of WT for feature extraction provides better precision compared with the research from Güler *et al.* [38]. In this approach, this model achieves a precision of 98.68% to classify epilepsy. Analyzing the computational complexity, Muñoz *et al.* [43] propose the implementation of WT with $O(n)$ time complexity, where n equals to the number of signal samples. On the other hand, ANFIS has the advantages of both fuzzy logic and ANN approaches. Still, it is computationally expensive and complex, typically $O(2^n)$, where n represents the number of data points to learn.

Hence, it is recommended only for scenarios with high computing resources availability [44].

Polat and Günes [45] propose a hybrid system based on Decision Tree (DT) and Fast Fourier Transform (FFT) for epilepsy detection. In this approach, the authors consider all five EEG time series available after Andrzejak *et al.* [37]. The proposal extracts 129 features from the EEG signal using FFT. Afterward, the authors apply this feature vector to train a DT model to detect epileptic seizures [45]. Furthermore, the training procedure considers cross-validation 10-fold.

The FFT is a well-known algorithm to compute FT in $O(n \log n)$ time complexity, where n equals to the number of samples of the input signal. The FFT performs better than classical Discrete Fourier Transform (DFT) algorithms with computational complexity of $O(n^2)$ [46]. For DT, Choromanska and Langford [47] propose an algorithm to train and test multiclass trees with $O(\log k)$ computational complexity with k equals to the number of classes. Concluding, the method from Polat and Günes [45] achieve an accuracy of 98.72% to classify epilepsy analyzing the EEG dataset from Andrzejak *et al.* [37].

In a new analysis, Polat and Günes [48] consider Welch FFT for feature extraction, Principal Component Analysis (PCA) for dimensioning reduction, and Artificial Immune Recognition System (AIRS) with Fuzzy resource allocation mechanism. The three-tier approach initially considered 129 features for classification, lately reduced to five remarkable characteristics after PCA application. In this analysis, the authors invest in cross-validation 10-fold and train-test split, considering 50%-50%, 70%-30%, and 80%-20% proportion.

This approach with Welch FFT, PCA, and AIRS achieve 99.81% of accuracy considering 50%-50% train-test split proportion and 100% for all other training strategies to detect epileptic seizures based on EEG data [48]. As discussed before, the computational complexity of the FFT computation is $O(n \log n)$, with n equals to the number of samples of the input signal. Dimensioning reduction applying PCA typically has computational complexity of $O(min[p^3, n^3])$ [49], considering that n is the number of data points and p equals to the number of features. Fuzzy Logic presents $O(2^n)$ complexity as discussed before.

Hosseini *et al.* [50] propose a binary classification for seizure detection considering normal individuals and epileptic patients. The authors propose a three-tier system and rely on the higher processing capabilities of the cloud servers to detect epileptic seizures in real-time. The system architecture considers *(i)* an iEEG sensor connected to a mobile device for data acquisition on the first tier; *(ii)* a set of notebooks or home-gateways performing feature extraction and classification on the second tier; *(iii)* A cloud server for big data processing on the third tier.

The iEEG enhances signal acquisition and is less prone to interference. It is an alternative to ambulatory EEG, as the latest is subject to errors due to noise, motion artifacts, and low conductivity in the scalp. Right after the data acquisition in the first

tier, the mobile phone transmits the EEG data to the connected home-gateway in the second tier. In the home-gateway, the signal flows through a filtering stage using WT, a dimensioning reduction applying Infinite Independent Component Analysis (I-ICA), and classification using Random Subspace with Support Vector Machine (SVM). This approach applies the ML algorithm in the second tier. Additionally, the system forwards the information to the third tier for further processing and data storage in the cloud center. This proposal from Hosseini *et al.* [50] achieve 95% of accuracy. As discussed before, WT complexity is $O(n)$. The algorithm for I-ICA dimensioning reduction is $O(KN)$, where K and N are the number of hidden sources and the number of data points, respectively. The implementation of SVM is kernel-dependent, and its time complexity is $O(n^3)$, where n equal the number of data points to classify [51].

De Cooman *et al.* [52] discuss the possibility of epileptic seizure detection using ECG instead of EEG. The ECG signal is easier to acquire compared to EEG, and an increase in the HR can indicate seizure for epileptic patients [52]. The earlier detection could alert the medical crew and the patient's relatives for immediate assistance. Thus, the authors propose an algorithm to detect Heart Rate Increase (HRI) based on single ECG and SVM for epilepsy classification. The dataset considers 127 complex partial and secondary seizures recorded from 17 patients.

The first step in the methodology by De Cooman *et al.* [52] is R peak detection from the ECG signal. Two consecutive R peaks define the HR. The detection algorithm computes the median of 15 consecutive HR to minimize the effect of small peaks. Then, inspects the gradient of 10 consecutive HR to compute the HRI. In the next step, the algorithm extracts the characteristic from the HRI, such as HRI peak, the time interval of the HR, and the maximum HR gradient. The approach considers the SVM algorithm, trained for all individuals in the dataset, but leaving one out for validation. This approach achieves an accuracy of 81.89% to detect epilepsy seizures. The algorithm to extract the HRI feature has a computational complexity of $O(n)$, where n is the number of HR measurements. However, the SVM algorithm has a computational complexity of $O(n^3)$, such as discussed before.

Vandercasteele *et al.* [53] explore the use of ECG and PPG sensors for epilepsy detection. This approach focuses on the accuracy and convenience of using wearable devices as an alternative to hospital equipment for long periods. The analysis considers the physiological information from 11 patients using wearable ECG devices and wrist-band PPG devices. The authors compare the results of their experiment with the sensitivity of an ambulatory ECG hospital system. The dataset counts for 701 hours of recording with 47 registered seizures.

The seizure detection methodology in Vandercasteele *et al.* [53] shares the same methodology from De Cooman *et al.* [52]. Additionally, the analyses submitted both Heart Rate Variability (HRV) and Pulse Rate Variability (PRV) to the detection algorithm. The evaluation criteria considered sensitivity, false positives per hour (FP/h), positive prediction value (PPV), and Receiver Operating Characteristics (ROC) curve. This approach achieves a sensitivity of 70% for wearable ECG sensor data, but only 32%

for PPG sensor data. Comparatively, the hospital ECG system achieves 57% of sensitivity.

In Neto *et al.* [20], the authors explore the application of classifier committee. In this ML technique, a classifier combines the results of other stand-alone classifiers to reach a resulting consensus. The authors explore the results for K-Nearest Neighbor (KNN), SVM, DT, Naïve Bayes (NB), and Random Forest (RF), with the Bagging algorithm implementing the committee. Neto *et al.* [20] reduces the dataset dimensionality using PCA to minimize execution time and memory consumption during the training-testing process. The analysis considers the Area under the ROC Curve (AuC) probabilistic performance indicator to evaluate the model‘s outcome. The AuC crosses the true-positive with the false-positive rates achieving results between 0 and 1. Thus, the higher the AuC better the model to correctly predict the outcome.

Initially, Neto *et al.* [20] manipulate the dataset to convert from time to frequency domain applying FT. The application of PCA reduces the dataset dimension by 91% to 270,002 attributes. Following, the authors provide a parameter grid for each stand-alone algorithm to come up with the best outcome. In this context, the KNN algorithm obtained the best AuC result of 0.5586. Classification using SVM achieves 0.5 with kernel function, DT achieves values around 0.7, and the NB algorithm trained with 10-fold cross-validation achieve AuC of 0.33. RF is a collection of DT and in this concept, Neto *et al.* [20] consider the forest with 1,000 up to 4,000 DT achieving AuC of 0.5279 with 3,000 trees. The classification committee approaches two scenarios. The first scenario concerns a homogeneous voting system combining KNN stand-alone results. The second scenario relates to a heterogeneous voting system combining KNN, DT, and NB results. The authors present that the homogeneous committee achieves AuC of 0.7486 and the heterogeneous committee achieves near AuC equal to 0.8

Table 3 summarizes the state-of-the-art analysis reported in this research work. It associates each proposal with their respective computational complexity. The computational complexity and feature selection are key factors determining the applicability of such ML algorithms in a wearable device context [54]. The computational complexity is directly related to the usage of scarce energy, computing, and storage resources of wearable devices.

Epileptic seizure detection application running on wearable devices context require low complex ML algorithms. This requirement copes with the device's limited processing capability, storage capacity, and battery lifetime. In this context, this analysis concludes that despite the excellent accuracy, not all ML investigated in related works fulfill the constraints imposed by wearable device systems. Besides, general architectures propose data transmission to the cloud servers. Thus, data transmission is an energy-demanding task subject to communication delays and interruptions.

Table 3: Comparison Between Different Machine Learning Algorithms to Classify Epilepsy

Author	Dataset	Algorithms	Complexity	Accuracy (%)	AuC
Güler *et al.* [38]	EEG [37]	RNN with LE	$O(n^3)$	96.79	–
Güler and Übeyli [42]	EEG [37]	WT ANFIS	$O(n)$ $O(2^n)$	98.68	–
Polat and Günes [45]	EEG [37]	FFT DT	$O(n\ lg\ n)$ $O(lg\ k)$	98.72	–
Polat and Günes [48]	EEG [37]	Welch FFT PCA AIRS with Fuzzy	$O(n\ log\ n)$ $O(min[p^3, n^3])$ $O(2^n)$	100.00	–
Hosseini *et al.* [50]	EEG [50]	WT I-ICA SVM	$O(n)$ $O(kn)$ $O(n^3)$	96.00	–
De Cooman *et al.* [52]	ECG [52]	HRI Extract SVM	$O(n)$ $O(n^3)$	81.89	–
Vandercasteele *et al.* [53]	ECG [53]	HRI Extract SVM	$O(n)$ $O(n^3)$	70.00	–
Neto *et al.* [20]	EEG	Classification Committee	–	–	0.7486

3.2 Traffic Prioritization

Typically, healthcare systems based on IoMT devices rely on a three-tier architecture: the body sensors, a communication gateway, and a cloud server. In such architecture, the body sensors and the communication gateway constitute an IoMT network. The cloud server provides a higher capacity for data storage and processing. The body sensors collect physiological data and transmit it through the gateway to the cloud servers using wireless, wireline, or a mixture of these two technologies. The network architecture and application scenarios were well explored in Kraemer *et al.* [10].

Hassan *et al.* [23] proposes the integration of Wireless Body Area Network (WBAN) and TCP/IP as communication technologies in an IoMT network transmitting to a cloud server. The authors address the packet loss problem adding an adaptive streaming method to adjust the network data rate based on the number of users and packet re-trans-missions. The concept behind Hassan *et al.* [23] consists of a four-layer architecture: perception layer, network layer, cloud computing layer, and application layer. The sensors constitute the most fundamental elements in the perception layer, transmitting data to the coordinator in the network layer. The coordinator operates with both Zigbee and TCP/IP protocols, sending data to the servers in the cloud computing layer. The proposal integrates a Content-Centric Network (CCN) to distribute the content to multiple destinations in the application layer. Each target application presents its requirements in terms of expected latency, bandwidth, broadcast or multicast capability, and other traffic characteristics. Simulations confirmed that this strategy reduces traffic delay and jitter to transmit a large volume of medical data in real-time.

The advances in medical therapies enhance the interest in QoS requirements for providing service to healthcare applications. Specifically, real-time applications such as human physiology monitoring, transmitting information through wireless medium access, require low latency network and energy-efficient protocols [55]. According to Yessad *et*

al. [55], different vital signs need different QoS, and the network design to address the requirements is challenging due to many factors. In this sense, that work surveys recent publications addressing QoS requirements and propose an analytical model to compare the system's performance. The authors enumerate the considerations for the design of an optimized QoS for the IoMT network. Notably, the authors discuss the challenges involving traffic types associated with heterogeneous sensor nodes, prioritization between the distinct traffic types, transmission delay, energy consumption, and attenuation in the transmission path.

Yessad *et al.* [55] analyses the research articles proposing multi-sink and single-sink approaches to address network reliability. Multi-sink protocols aim to improve network reliability for sending the data packets to several sinks. Single-sink protocols apply multi-hop routing alone or combined with single-hop to enhance reliability. The surveyed articles proposing multi-sink protocols define two or more priority queues to transmit data. The proposals with single-sink protocols focus on latency reduction identifying the best route for the traffic and seeking energy-efficient strategies. Finally, Yessad *et al.* [55] applies the Markov chain to compute the probability of route rupture and transmission success of each model. The authors conclude that multi-sink approaches supersede single-link proposals when reliability and transmission delay improvement are critical aspects.

The continuous transmission of physiological data originated in wearable devices faces some constraints. Restrictions associated with interference, collision, and bandwidth limitation increases the competition for medium access in the wireless network. Hence, transmitting only relevant information for clinical diagnostic constitutes an alternative to bypass the restrictions. In this context, Vergütz *et al.* [17] analyses the statistical information carry on the physiological data to send an alerting beacon to a cloud server. Such analysis aims to prioritize the transmission of the medical alert.

The proposal in Vergütz *et al.* [17] considers a system architecture with three stages. In the first stage, a group of wearable sensor devices attached to the patient's body collects physiological information. A coordinator in the second stage accounts for receiving data from the body sensors and process it locally. Finally, in the third stage, the coordinator sends the medical alerts to a WiFi access point to reach the healthcare center. The data processing in the second stage performs a statistical analysis of the physiological data and identifies respiratory frequency alteration in patients suffering from pulmonary edema. This work considers the return rate, autocorrelation, variance, asymmetry, and kurtosis as relevant statistical indicators for such an analysis.

After identifying the respiratory frequency alteration, the coordinator needs to transmit the alerting beacon in near real-time to the healthcare center. However, the transmission in the WiFi network offers few QoS possibilities as explained in Section 2. Specifically, the IEEE amendment prioritizes voice and video over other traffic types. In this context, medical alerts do not have any specific transmission queue to grant prioritization. The proposal in Vergütz *et al.* [17] combines the IEEE 802.11 EDCA access category to provide higher priority to the medical alert. Precisely, the authors propose a new access category referring to medical alarms. Thus, for this new access category,

they reduced the interframe interval and contention window in the WiFi network. Hence, medical alerts gain more airtime when compared with voice and video data packets.

The investigation of QoS metrics for healthcare applications is the subject of research for Park *et al.* [21]. The authors discuss the influence of the packet error rate in the wireless network transmission for the applicability of the received signal for the diagnostic purpose. Specifically, the error rate cause missing packets, missing packets cause signal distortion, and this aspect impact negatively the received signal. Moreover, the distorted signal may not carry enough information for the healthcare application to conclude its clinical diagnosis. In this context, Park *et al.* [21] proposes a QoS metric for an ECG system transmitting data through a wireless network. Hence, the authors quantify the preserved diagnostic information perceived at the receiving end of the transmission.

The starting point for Park *et al.* [21] research defines the maximum latency allowed for medical applications in the context of a hospital network. In this scenario, traffic type ranging from diagnostic telemetry to guest access in the hospital network accepts delay between 200ms to 1s. To define an alternative metric, the authors consider the main characteristics of an ECG signal for medical analysis. Initially, the proposal defines feature vectors representing the original and the received signal. Then, this work computes the weighted diagnostic distortion as a factor of the normalized difference vector and the diagonal matrix of features weights. Finally, the authors simulated the model using three ECG features, named, RR interval, QRS+ amplitude, and QRS- amplitude, with a weighted diagonal matrix equal to [2 2 2]. The research conclusion indicates an essential difference between the packet error rate and the medical QoS metric, requiring more research efforts in the subject area [21].

In practical applications, most of the internet traffic occurs in bursts. In this scenario, a certain level of congestion affects the network QoS in some moments. Patel and Choudhary [56] study the traffic delay over congested WLAN 802.11n in the context of video transmission prioritization. Specifically, this research manipulates the access categories queues in the EDCA Qos method. The research from Patel and Choudhary [56] proposes a cross-layer mapping to provide QoS for video stream employing EDCA function..

In the 802.11 networks, the heavy traffic scenarios cause packets discarding. Specifically, if any of the access categories queues run out of capacity, implicates new incoming packets to be dropped. The cross-layer mapping algorithm proposed in Patel and Choudhary [56] dynamically accommodates the video packets to an empty access category queue in the advent of network congestion. The proposal consists of retrieving the I/P/B video slice from the Medium Access Control (MAC) layer and distribute the information in three of the access categories queues according to the congestion levels. The I-frame always goes to the video queue. The cross-layer algorithm diverts the P/B-frame to the best effort and background queues once the video queue is congested. The authors evaluate this proposal considering the end-to-end delay, throughput, and Packet Signal-to-Noise Ratio (PSNR). The researchers conclude that adaptive cross-layer mapping performs better than the static cross-layer in terms of delay, jitter, and PSNR.

Many applications share the same frequency spectrum, and a certain level of interference in the network transmission is expected. For instance, ZigBee and IEEE 802.11 channels overlap operating at 2.4 GHz. In this context, the higher power level from the WiFi causes ZigBee channels to back off [12]. ZigBee technology provides connectivity between the medical body sensors and a gateway. The gateway aggregates the information from various medical body sensors and forwards the data to a health monitoring system through a WiFi access point. The access point concentrates traffic from the medical body sensors and background devices, such as internet navigation, file transfer, peer to peer connection, and audio and video streamings. The proposal from Kim *et al.* [12] consider delaying background network traffic to increase the QoS for medical data streams. The strategy implementation proposes an algorithm to minimize the traffic generated on delay-tolerant applications.

In the proposal from Kim *et al.* [12], the algorithm classifies WiFi traffic into real-time and non-real-time. In this context, real-time traffic includes voice and video call transmissions, while non-real-time includes peer-to-peer and video streaming transmissions. The algorithm extracts traffic characteristics from each transmitting node using Wireshark - an open-source packet analyzer - then computes the statistical features based on frame size and interarrival time. Furthermore, the algorithm computes the channel busy-period, and the WiFi access point sends a control message to non-real-time nodes to back off the transmission. Hence, the algorithm grants ZigBee nodes with the appropriate airtime to transmit physiological information.

Sodhro *et al.* [16, 57] investigate methods to provide QoS for medical applications. In Sodhro *et al.* [16], the authors propose a window-based rate control algorithm for medical video. Specifically, this work analyses the scenario of a surgery video transmission over a 5G network. Additionally, the authors considered an edge computing framework to optimize communication. In such an analysis, the authors investigated the network metrics such as standard deviation, peak to mean, delay, and jitter balanced with client buffering size and window size to optimize the QoS.

In Sodhro *et al.* [16], the authors explore the concepts for mobile edge computing in Matlab. The testing considers a pre-recorded medical video with 8 seconds duration encoded with MPEG-4. In this experiment, the authors examine a single-hop network. Based on the results, this analysis concludes that delay and jitter increase with the increase of the client buffer. However, peak-to-mean and standard deviation decrease, pointing out to a smooth transmission of the medical video. The authors propose an algorithm performing better than the baseline algorithm tested with 600 frames for window size or 20-sec playback delay.

Afterward, Sodhro *et al.* [57] proposes an Adaptive Quality of Service Computational Algorithm (AQCA) that relies on monitoring performance indicators, combined with QoS adaptation in the physical, MAC, and network layers. The authors motivate the discussion in terms of the patient's perceived quality of experience. In this sense, this work considers emergency conditions and regular patient monitoring requiring different bandwidth for data transmission. Hence, the authors correlate the QoS metric, *i.e.*,

transmission power, duty cycle, and route selection, with the Quality of Experience (QoE) perceived by end-users concerning ECG processing.

Al-Turjman *et al.* [8] survey the IoMT solutions and propose a generic framework based on a three-tier approach: *(i)* data acquisition, *(ii)* communication gateway, and *(iii)* cloud server. In this survey, the authors classify the IoMT applications in body-centric and object-centric, for both indoor and outdoor usage case. Body-centric application refers to scenarios where sensors directly connected to the human body collect physiological information - wearable devices. The complementary, object-centric application enhances the IoMT user experience without any direct connection with the human body but providing solutions such as mobile Intensive Care Unit (ICU).

In the context of Al-Turjman *et al.* [8] analysis, the data acquisition includes aspects of sensing devices, signal pre-processing, and Analog/Digital conversion. Following, the authors define the IoMT gateway as both physical devices or software-defined solutions to interconnect the data acquisition tier with the cloud server. In this sense, the gateway provides data normalization, data pre-processing, and network connectivity. The cloud server executes most of the data mining tasks [8]. Investigating the published articles, Al-Turjman *et al.* enumerate the main challenges in the IoMT applications, named, the increasing healthcare costs with the introduction of new technologies, the signal acquisition quality to avoid any misguiding information, the data security and individual's privacy, the device's safety to minimize the risk of accident, energy consumption, and device's comfortable usage. These challenges lead to several opportunities for exploring in future works. We highlight the opportunities in the area of machine learning for a decision support system and the employed communication technology.

Table 4 summarizes some related works in the literature. Based on the analysis of the state-of-the-art, the present works investigated QoS in the context of IoMT, Low Power Wide Area Network (LPWAN), and WiFi networks. However, these works they handle the transmission of only one physiological stream. To the best of our knowledge, our study is the first to evaluate a machine learning staging to classify multiple vital signs data streams and apply the classification information to prioritize the transmission across the network.

3.3 Chapter Conclusion

The application of ML algorithms for clinical diagnostic gain momentum with the introduction of new technologies. Nevertheless, the analysis of physiological data such as EEG, ECG, and PPG for epileptic seizure detection is not recent. As noted in related works, most proposals achieved high accuracy with low false alarm rates. However, the implementation strategies do not privilege the application scenario with scarce computational resources.

In the context of IoMT network, it is essential to investigate the computational complexity of the implemented proposal. The ML algorithms for classification required

Table 4: The summary of data traffic classification to network access priority for Health-Care applications

Work	**Network Architecture**	**Metric**	**Description**
Hassan *et al.* [23]	WiFi + LPWAN	Packet Loss	Adaptive streaming based on the number of devices
Patel and Choudhary [56]	Congested 802.11n	Delay	Cross-layer mapping to provide QoS for video streams
Kim *et al.* [12]	WiFi + LPWAN	Delay	Delay background network traffic to provide QoS for medical data streams
Vergutz *et al.* [17]	WiFi + LPWAN	Delay	Send alerting beacons using EDCA in WiFi
Sodhro *et al.* [16]	5G	Delay Jitter	Window-based rate control algorithm
Sodhro *et al.* [57]	WiFi + LPWAN	Bit Error Rate Jitter Throughput Delay	Adaptive QoS computation algorithm

that new data exhibit lies within the same range of training data. Any other situation will lead to unpredictable results. Hence, the new exhibit may cause algorithms to lose generalization capability. Thus, the algorithm requires periodic training and updates to keep the analytical capacity. In this sense, the combination of high accuracy algorithms with low computational complexity solutions demands more investigation in the IoMT context.

The related works reviewed in this research analyses aspects involving an IoMT network. The typical architecture involves the body sensors, the communication gateway, and the cloud servers. In this scenario, ML algorithms have the potential applicability in the communication gateway or the cloud servers. The application scenario includes clinical diagnostic or communication optimization to provide medical devices with a better QoS. However, little research works investigate the ML applied with multiple physiological streams and transmission prioritization based on the relevance of the vital sign to the clinical diagnostic.

As discussed in the related works, the medical application has strict QoS requirements. The analyzed works propose solutions to reduce packet delay, packet loss, bit error rate, throughput, and jitter. Additionally, the researches investigate the issues involving available technologies such as LPWAN, WiFi, BLE, NFC, and others. However, the analyzed works mostly considered the transferring of a single physiological stream, which diverts from a practical application. Patients in chronic conditions monitored outside hospital premises likely require the transmission of more than one physiological stream. Hence, the investigation to provide QoS for IoMT applications must evolve to scenarios of multiple physiological streams competing for the wireless medium access.

CHAPTER 4

Performance of Machine Learning Algorithms for Epileptic Seizure Detection

This Chapter introduces a proposal to answer the first and second research questions. Specifically, we investigate the ML algorithm's applicability to detect epileptic seizures. Additionally, we evaluate the algorithm's computational complexity and precision in fulfilling the research objective in a IoMT context. Moreover, we investigate the application of an ensemble to combine the results of stand-alone classifiers. Section 4.1 describes the application scenario and the main building blocks of our proposal. Section 4.2 introduces the dataset considered in our analysis. Section 4.3 discusses the characteristics of six of the most common machine learning algorithms for classification. Following, Section 4.4 discusses the accepted metrics to evaluate the machine learning algorithms applied for classification. Finally, we present and discuss our results in Section 4.5, and point for future research directions in Section 4.6.

4.1 Overview

People with epilepsy require frequent monitoring and ambulatory EEG constitute a practical clinical test to detect seizures [26]. However, it is unfeasible to use ambulatory EEG equipment outside the hospital premises. In this context, we consider the possible use of wearable devices to collect the patient's vital signs outside the hospital premises. Hence, the brain activity is the principal physiological information for epileptic seizure detection. Moreover, the wearable device and a body gateway or smartphone to coordinate transmission and process data constitutes the IoMT systems' backbone. In this sense, data processing includes signal normalization, feature selection, and seizure detection. Hence, the monitoring system may transmit only the seizure detection information instead of the

complete EEG signal.

There are already some wearable options in commercial use capable of collecting EEG signals. Bioserenity is the startup company behind the NEURONAUTE project [1]. The project develops a textile to collect EEG information, implementing the 10-20 electrodes placement, and connecting to a mobile application to provide 24-hour monitoring. Behind-the-ear electrodes constitute an alternative to collect EEG data for patients suffering from focal epilepsy [58]. Gu *et al.* [58] demonstrates that SVM combining EEG features obtained with behind-the-ear electrodes achieve lower accuracy than scalp EEG systems; however, the solution delivers a lower false alarm rate. Another potential option to collect EEG data is the e-tattoo patented by Motorola [4].

In Chapter 3, we discuss the use of ML to analyse vital signs and detect epileptic seizures. For the scenario of IoMT applicability, we analyze the performance of six machine learning algorithms following the workflow outlined in Figure 6. To simulate the sensor data collection, we read the EEG data from a CSV file. After reading the information and storing it in a data frame, we normalize the dataset using the minimum and maximum values. Specifically, we scale the values according to the observed minimum and maximum values in the dataset, calculating the new value according to Eq. 4.1. Following, we split the dataset into three equally-sized subsets for training, testing, and validation. We apply the training and testing subsets to configure individual ML models and reserve the validation subset to validate an ensemble model. Furthermore, the ML model requires a characteristic (*i.e.*, feature) to express mathematically. For this analysis, we select the amplitude of the waveform in the time domain as characteristic for modeling. After data preparation, we trained six machine learning models, namely, DT, RF, KNN, NB, ANN, and SVM using cross-validation 20-fold with the corresponding training set. Afterward, we tested the model's accuracy submitting the testing subset to the trained model. Finally, we apply the predictions in the testing set and use it to train an ensemble model. We validate the ensemble model using the validation set.

$$normalize(x) = \frac{x - min(x)}{max(x) - min(x)} \tag{4.1}$$

4.2 EEG Dataset

For the sequence of this analysis, we consider the EEG dataset available at the University of California at Irvine (UCI) ML repository [59], derived from Andrzejak *et al.* [37]. This dataset is composed of five classes denoted from 1 to 5, as shown in Table 5. The EEG signal collection considered both epileptic patients and healthy individuals. Epileptic patients were in presurgical evaluation. In this condition, patients received intracranial electrodes placed in both the epileptic zone and in the opposite brain hemispheres. For healthy individuals, the EEG acquisition adopted the international 10-20 system to place

[1] https://www.bioserenity.com/en/

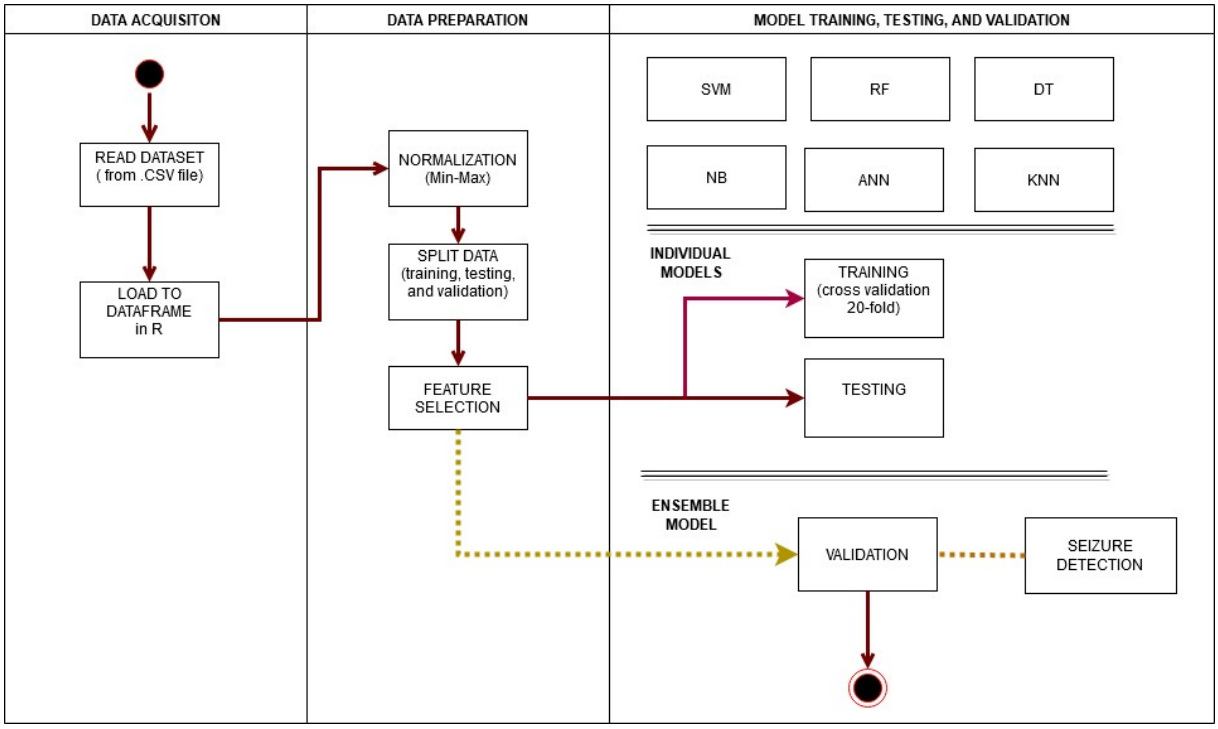

Figure 6: Diagram for the proposed modeling

the electrodes on the scalp. That work reports that individuals were awake and relaxed during recording. In this context, classes 1 and 2 refer to epileptic patients recorded during a seizure and seizure-free period. Class 3 relates to epileptic patients recorded with the intracranial electrode placed in an epileptic-free zone. Classes 4 and 5 refer to healthy patients registered with their eyes closed and eyes open, respectively. Concluding the analysis, only class 1 contains the seizure activity.

Initially, a total of 500 individuals took part in the data collection, having their respective EEG time series saved in 5 different folders with 100 files each. Thus, each set composing a class contains 100 single-channel of EEG segments with a duration of 23.6 seconds sampled in 4097 data points. The EEG segments constitute samples from a continuous multi-channel EEG recording, from healthy volunteers and epileptic patients, selected by a specialist after visual inspection. The UCI ML repository reorganized the dataset in a single comma-separated values (CSV) file to simplify the access. The instances in the simplified dataset count for 1-second of EEG sampled in 178 points, with each point representing the signal's amplitude value at that moment in time. In this reorganization, the UCI ML repository provided a file with 11500 examples of EEG data, each pattern with 178 data points representing the amplitude value. Additionally, the UCI ML included the corresponding class (1, 2, 3, 4 or 5) in column 179 [59].

The EEG registers a distinctive discharge during epileptic seizures. The spike-and-wave pattern in the waveform generalizes most of the epileptic syndromes [26]. In this context, a peak lasting from 20 msec to 70 msec or a sharp wave between 70 msec and 200 msec has strong characteristics during EEG visual inspection. This characteristic is remarkable when comparing the waveforms from seizure and seizure-free EEG signals,

Table 5: Classes on EEG dataset

Class	Description
1	Recording of EEG data during seizure activity
2	Recording of EEG data from tumor area
3	Recording of EEG data from healthy brain area
4	Recording of EEG data while patients had their eyes closed
5	Recording of EEG data while patients had their eyes open

as seen in Figure 7 exemplifying the classes 1 and 5 from Table 5. Using a ML approach enhances physical survey capabilities. In this sense, the ML model seeks to map the features that identify the seizures. The right combination of features and algorithms improves the model's accuracy. However, noise, motion artifacts, and sensor calibration data cause interference in the collected signal, distort the characteristics, and inaccurate the model.

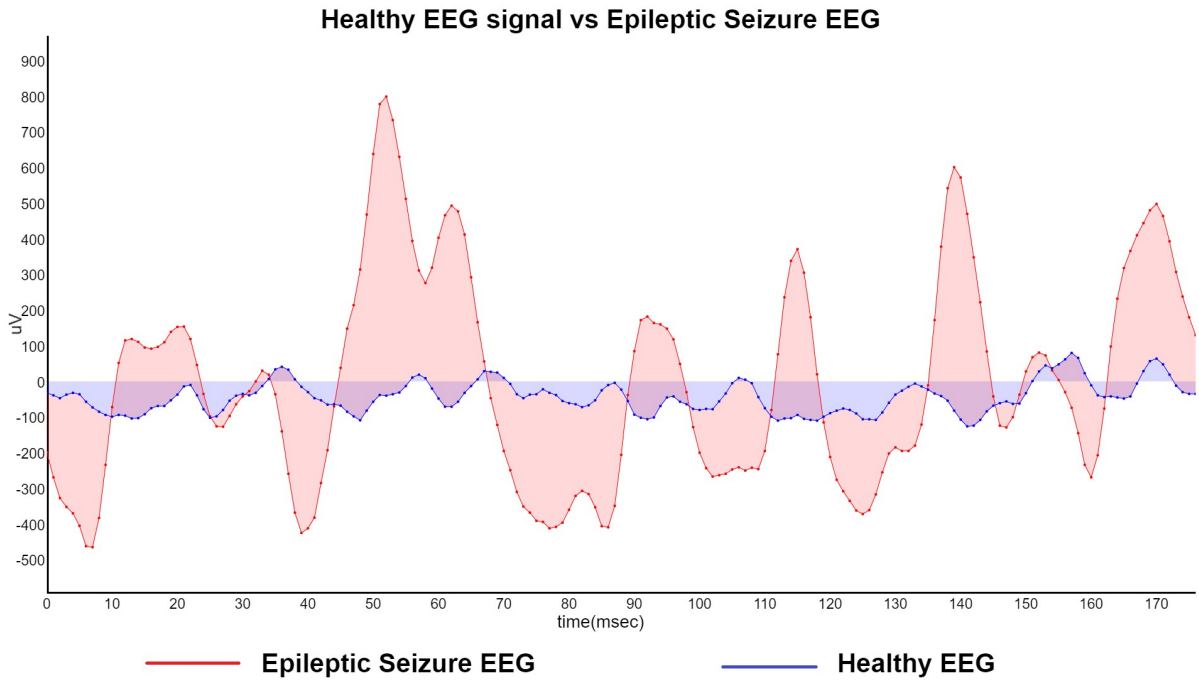

Figure 7: Comparison of Healthy EEG signal with Epileptic EEG signal during seizure

To filter the imperfections that noise causes in the EEG signal, some research authors choose to decompose the time series in its spectral frequency components. In this context, power spectral density, the frequency with maximum and minimum amplitude, spectral entropy, band energy, and discrete wavelet transform coefficients constitute feature options in the frequency domain [60]. However, transforming from time to the frequency domain requires additional computational effort. In the context of IoMT, any transformation inserts computation that drains energy from the devices. Using time-domain features is more straightforward. In this sense, minimum and maximum value, mean, variance, standard deviation, percentiles, and the number of positive and negative

peaks constitute potential feature options.

In our research, we evaluated a set of ML algorithms in the time domain, using the amplitude of the waveform as the classification feature. We proposed the evaluation in the time domain to avoid additional processing effort to obtain features in frequency or time-frequency domains. In our favor, we acknowledge that Andrzejak *et al.* [37] removed the discontinuities from the original EEG time series. Thus, the authors eliminated the inaccuracies caused by noise and motion artifacts. Additionally, the UCI ML repository provided a cleaner dataset by reducing the instance size from 23.6 sec to 1 sec [59].

As discussed in related works, epilepsy syndrome affects from 0.4% to 1% of the world population [24]. The authors using the dataset from Andrzejak *et al.* [37] propose solutions using balanced data, *e.g.*, combining two, three, or the five classes with equilibrium in the number of instances in each class. Considering we have more healthy individuals than people with epilepsy, it is more realistic to train the ML model to identify epileptic seizures under an imbalanced dataset. In this context, our proposal investigates the solution under an imbalanced dataset proceeding with a binary classification using the categorical class as follow:

- **Seizure**: Refers to EEG waveforms identified by an expert as exhibiting an epileptic seizure (Class 1 from UCI dataset [59]).
- **Non-Seizure**: According to the expert evaluation, it relates to the EEG waveforms from healthy individuals or epileptic patients during seizure-free intervals (Classes 2 to 5 from UCI dataset [59])

4.3 Machine Learning Algorithms

ML algorithms constitute a proven methodology for pattern recognition. Hence, ML can be an efficient procedure for the clinical evaluation of patients with epilepsy. ML provides accurate diagnostic given the right features and input pattern. In this context, EEG provides the input pattern for analysis, and the spike-and-wave characteristic in the waveform gives the feature for epileptic seizure detection. In our modeling, we trained individually six ML algorithms, namely, DT, RF, KNN, NB, ANN, and SVM. After, we tested and identified the seizures on new data. Following, we use the outputs from the six ML to train an ensemble model. Finally, we validated the ensemble model.

4.3.1 Decision Tree

DT became a popular machine learning classification method due to its versatility and applicability to many problems, ranging from object identification to medical diagnostics. The concept is to use the tree structure to split features into different classes based on probabilistic criteria and numeric threshold. Features or attributes define the

class, *e.g.*, formats and sizes of objects, or medical symptoms like pain and fever. There are many algorithms to grow a DT, such as Iterative Dichotomiser 3 (ID3), Classification and Regression Tree (CART), Chi-squared Automatic Interaction Detector (CHAID), and C5.0 - an alternative to ID3.

DT has the advantage of being easier to interpret compared to other classification methods, such as ANN and SVM. However, the model may lose generalization capacity due to overfitting. Specifically, the algorithm will stop only when all data are classified, and depending on the features, this whole process can cause overfitting. There are two common ways to deal with the overfitting effect: limit the number of branches or allow a new ramification only with a minimum number of data points to fill in the new division.

An essential aspect of the DT configuration is how to define the importance of each feature to maximize the classification results. The algorithm takes the characteristic that better represent the class and position it in the root. The literature proposes some indexes to identify the most relevant features: the Gini Index, Entropy Index, and Information Gain are indexes examples. Gini index expressed in Eq. 4.2 is a measure of the variable's importance for the dataset. The Entropy Index showed in Eq. 4.3 is a measure of uncertainty associated with the variable. The information gain measures the information obtained by observing one random variable based on the observation of another random variable. Specifically, the information gain from a variable A expresses the reduction of entropy of that variable based on the learning of a variable B state (Eq. 4.4).

$$Gini(S) = 1 - \sum_{j} p_j^2 \tag{4.2}$$

Where S is the dataset and p_j is the relative frequency of class j in S.

$$H = -\sum_{i=1}^{N} P_i \, log_2 \, P_i \tag{4.3}$$

With P_i the probability of the value i to occur and N is the number of possible values.

$$Gain(A) = H(B) - H_A(B) \tag{4.4}$$

We follow the implementation of the C5.0 algorithm available in the caret package in the R language. This algorithm requires a categorical class to classify the data correctly. The C5.0 model selects the feature with higher information gain to place the sample in the tree root. After finishing splitting data in the tree, the algorithm reevaluates the lower leaves and removes those with less critical information.

4.3.2 Random Forest

RF is a collection of DT trained with randomly selected data. Hence, the algorithm guarantees that each tree is slightly different from each other. Thus, each tree may return a distinct result for a given dataset. The RF algorithm classifies the data based on a voting system involving the results from the individual trees. Specifically, direct voting count how many trees classified a given feature under a particular class. Additionally, weighted voting returns the ratio of elements belonging to a given group.

RF performs better than DT in two aspects, namely, overfitting and anomaly detection. During the RF training process, the outliers will be present in some of the trees but not in all of them, and thus the voting system guarantees the anomalies will be isolated. The voting system also minimizes the effect of overfitting concerning the individual decision tree. However, RF has problems to extrapolate data. Specifically, attribute values in the validation set must be within the value limits of the training set. Not trained or out-of-limit attributes may lead to unpredictable results when included in the validation set.

The RF algorithm accepts the number of trees to grow as a configurable parameter. There is no best value, and the limit should be the storage capacity to save the DT. However, the higher number of DT does not necessarily pay off in the classification results. The right approach is to start with a few trees and gradually increase their number until the benefit does not worth the resources.

4.3.3 K-Nearest Neighbor

KNN classifies data based on the distance, usually Euclidean distance, between a particular data point and its k neighbors. The KNN algorithm has a great heritage of possible applications, such as meteorological prediction [61], elderly fall detection [18], crime detection [62], epilepsy seizures detection [63], and many others. KNN has the advantage of making no initial assumption about the data set because it merely groups the data points based on similarity with historical data. Differently from the other models discussed in this work, KNN does not require training. However, the algorithm stores all instances in the dataset and only stops after grouping all data. Usually, but not always, it achieves better accuracy with higher k values.

4.3.4 Naïve Bayes

The NB algorithm derives from the conditional probability theory [64], where NB associates the probability of an event B to occur based on previous knowledge of an event A, as shown in Eq. 4.5.

$$P(A|B) = \frac{P(A) * P(B|A)}{P(B)} \tag{4.5}$$

In the BAYES theorem, $P(A)$ is the **Priori** probability known to be true. $P(B|A)$ is the **Likelihood**, the conditional probability given that new data is known to be true. $P(B)$ is a **Normalizing Constant**, to guarantee that probabilities will sum 1. $P(A|B)$ is the **Posteriori** probability, obtained after incorporating new data to the calculations and after normalization. The NB algorithm maximizes the **Posteriori** probability. The algorithm initializes the probabilities for the outcome variables and adjusts it in each interaction based on what happened with the other variables in the dataset.

4.3.5 Artificial Neural Networks

ANN are machine learning algorithms capable of classifying linear and non-linear data. The typical ANN architecture presents a given number of connected neurons arranged in layers. The data structure represents an artificial neuron, usually configured with pointers connecting to other neurons and a weight value (real number) to ponder each connection.

Multi Layer Perceptron (MLP) refers to an ANN configured with a variable number of neurons arranged in one input layer, one or more hidden layers, and one output layer. Specifically, MLP propagates a stimulus injected into the neurons on the input layer, through the connected neurons in the hidden layers, and reflects in the output layer. Back Propagation is a common training algorithm for MLP that executes in two phases:

- **Forward phase:** initially, each neuron receives a fixed weight value. The algorithm transfers the injected signal from the input layer to the output layer using the weights to ponder the result.
- **Backward phase:** the algorithm calculates the error between the obtained and desired outputs and back-propagates the error in the network, adjusting the neurons' weights in the way back.

The training process repeats the forward and backward phases for a certain number of interactions. In each interaction, the algorithm focus on minimizing the error between the actual and the desired output. The training process stops when the error falls below a threshold, or the algorithm reaches the maximum number of interactions.

4.3.6 Support Vector Machine

SVM is a ML algorithm based on the concept of kernel. Haykin [65] defines the kernel k of a input vector x, denoted as *k(x)*, as the function with similar properties of a probability density function, such as described below:

- property 1: the kernel *k(x)* is a real function of x, starting in its maximum value, symmetric, continuous, and bounded.

- property 2: The total volume under the surface of the kernel *k(x)* is unity.

The concept behind SVM is to construct a hyperplane to work as a decision surface to separate patterns. The SVM algorithm extracts a small set from training data to work as a support vector and compute the inner-product kernel between the support vector and the input data set vector.

4.3.7 Ensemble Classifier

In practical life, there are several circumstances where experts diverge in their opinion about a subject. Differences in skill levels and experience, among other reasons, lead to such disagreement. For mission-critical decision making, it is reasonable to use established criteria to reach a consensus, *e.g.*, a voting system. The classification committee also referred to as ensemble classifier, is the ML implementation of this concept [20, 66].

When training stand-alone models, every single one might perform better for a specific set of features or adapt better for the problem in focus. The ensemble classifier composes a broader resolution combining the solution from stand-alone ML models. This implementation potentially enhances system performance since the final solution combines the majority prediction from individual results. Bagging, boosting, and stacking are the most adopted strategies to implement the ensemble model [67]

The Bagging and Boosting strategies combine the results using a voting system. These two strategies converge using stand-alone models of the same type. However, they diverge in the voting system. On the one hand, bagging uses simple voting considering the same weight to every prediction. On the other hand, the boosting strategy biases the voting system giving more weight to models with higher accuracy. The training set for the ensemble model using bagging or boosting derives from the training set used for the stand-alone models. The algorithm selects some, but not all, instances from the training set through a random procedure. Thus, the derived training set counts for duplicated and omitted examples when compared with the original dataset.

The Stacking strategy applies to stand-alone models of different type, *e.g.*, combining tree, probabilistic, and kernel solutions. To implement this strategy, we start defining the stand-alone models individually. Following, we enrich the dataset with the predictions of these stand-alone models to create a new dataset. Finally, we apply the new enriched dataset to train the ensemble classifier. This strategy brings more benefits when the stand-alone models are not correlated. Considering the stand-alone models do the inferences, makes sense that the ensemble model applies a simple algorithm like linear or tree model to combine the results.

4.4 Evaluation Metrics

A paramount aspect of any ML model is its performance according to different indicators. In other words, is measuring how good the model is in achieving its objective comparing with the chance. For classification, the metrics derived from the results presented in a confusion matrix as an exhibit in Table 6. A confusion matrix crosses the predicted with observed values, considering the model's performance in classifying unseen data [68]. The confusion matrix tabulates the predicted results against the observations. Specifically, True Positive (tp) stands for correctly accepted instances, False Positive (fp) relates with incorrectly accepted instances, True Negative (tn) refers to correctly rejected instances, and False Negative (fn) computes the incorrectly rejected instances. Based on the confusion matrix, we derive Key Performance Indicators (KPI) for the model, such as Precision-Recall, Accuracy, Sensitivity, Specificity, and Kappa.

Table 6: Confusion Matrix

		OBSERVED	
		A	B
PREDICTED	A	true positive (tp)	false negative (fn)
	B	false positive (fp)	true negative (tn)

Precision considers the number of attributes correctly classified to a given class compared to the number of characteristics correctly and incorrectly classified to that class, which is computed based on Eq. 4.6. Precision measures the classifier's correctness and the relevance of positive classifications. Higher precision means a higher number of true positives and a lower number of false positives.

$$Precision = \frac{tp}{tp + fp} \tag{4.6}$$

The recall complements the understanding from precision. Recall expresses the fraction of relevant instances retrieved by the model as an exhibit in Eq. 4.7. Specifically, recall is the ratio of correctly predicted positive to the total number of expected positive observations.

$$Recall = \frac{tp}{tp + tn} \tag{4.7}$$

Accuracy has a slightly distinct understanding of precision. Accuracy is the relation between the correct classified instances (positive and negative) of the problem over the total number of instances. Thus, accuracy includes the true negative value to the equation of precision and calculate not only the true positive. Hence, the accuracy

expands the calculation of precision, as expressed in Eq. 4.8.

$$Accuracy = \frac{tp + tn}{tp + fp + tn + fn} \tag{4.8}$$

Sensitivity and specificity complement the understanding of accuracy and precision. The sensitivity is the true positive rate and relates the accurate positive predictions with positive observations, computed based on Eq. 4.9. Sensitivity quantifies how good the model is in avoiding false negatives. The specificity does the same for the false positives. Specificity means the rate between accurate negative predictions and negative observations, as shown in Eq. 4.10. It refers to how good a model can be in minimizing false alarms.

$$Sensitivity = \frac{tp}{tp + fn} \tag{4.9}$$

$$Specificity = \frac{tn}{tn + fp} \tag{4.10}$$

Additionally, the Kappa normalizes the Accuracy results with a chance. In this sense, Kappa compares the observed accuracy with the expected accuracy if the classification results occurred by chance, as expressed in Eq. 4.11. Note that Kappa will always return a value between 0 and 1.

$$Kappa = \frac{ObservedAccuracy - ExpectedAccuracy}{1 - ExpectedAccuracy} \tag{4.11}$$

4.5 Results and Discussion

The body sensors, the communication gateway, and the central server constitute the main building blocks in the IoMT architecture [10]. The body sensors collect the physiological data but have a low computational capacity to perform complex tasks. The communication gateway intermediates the body sensors connections and manages the traffic to reach the central server. Finally, the central server with higher computational capacity process most of the analysis to support the medical crew.

To embed an ML technique in an IoMT architecture requires both model's accuracy to execute its purpose and capacity to minimize the false alarms (false negatives and false positives). In this context, a single ML metric is not suitable to fulfill this analysis. Hence, the discussed ML metrics for classification complement each other. Thus, we initially analyze the results based on Accuracy and Kappa, according to Figures 8 and 9, respectively.

Examining the accuracy outcome in Figure 8, we observe that results are statistically equivalent. First of all, we apply the same dataset for all investigated algorithms.

Following, we consider the significance test between each pair of models to compare the results. In this context, we verify that the resulting variance between models spans zero, *i.e.*, it is not statistically relevant. For instance, the results for SVM and RF models vary 1.44E-05 when calculating the significance test, which is near-zero variance. Besides, we consider the confidence level of 95% for all models. The confidence level expresses the trust that reproducing the experiment with different data exhibits achieves the same result. Notably, the SVM and RF models achieve the highest accuracy for the EEG dataset. On the one hand, the SVM with radial kernel reaches 97.26% accuracy. On the other hand, RF achieves 97.08% for the same dataset.

Training the SVM is kernel-dependent. In the worst-case scenario, Abdiansah *et al.* [51] demonstrates that SVM has $O(n^3)$ complexity with LibSVM implementation for both training and prediction. Therefore, the cubic computational complexity becomes challenging in an IoMT architecture. The RF model performs well for small datasets, but implementation complexity increases in scenarios with high data volumes. Hence, Choromanska and Langford [47] propose an algorithm to train and retrieve information from the trees with $O(log\ n)$ complexity. Thus, to grow a forest turns the computational complexity to $O(n\ log\ n)$. For both SVM and RF computational complexities, n represents the dataset dimension.

The DT model achieved an accuracy of 96.66%, with 95% of confidence level. As discussed before, Choromanska and Langford [47] propose an algorithm with $O(log\ n)$. However, the DT algorithm is less performing concerning outliers in the dataset compared to RF. Alternatively, the NB model reaches 95.98% of accuracy. This result is 1.10% below the accuracy result achieved by RF. Nevertheless, the NB model has the advantage of being simple to train and recover. Ahmadi and Bouallegue [69] establish that the NB computational complexity is equivalent to $O(mn)$, with m equals to the number of features and n equals to the number of instances. Thus, the computational complexity for NB bounces between linear to quadratic, depending on the problem dimension.

The ANN model achieves an accuracy of 93.53% when trained with backpropagation with a single hidden layer. Backpropagation is a popular ANN training algorithm, but backpropagation may converge to a local minimum, and thus the result may not reach the optimum value. Therefore, the ANN requires frequent training revision to enhance generalization capability when it starts lacking accuracy. Bilski *et al.* [41] explains that training a neural network with an optimized algorithm such as Levenberg-Marquardt is equivalent to $O(n^2)$ using parallel processing. However, the prediction using an ANN requires just a multiply operation, which is straightforward to fulfill. In this context, the computational complexity to train the ANN is time-consuming from the application perspective, but the ANN method has advantages during prediction.

Comparatively, the KNN algorithm groups the nearest neighbors to the k initial centroids using a distance metric, *e.g.*, euclidian distance. Calculating the arithmetic distance between the new data sample and the centroids is a linear operation. However, the algorithm is space-consuming since it tries to accommodate all dataset instances in the model up to the limit of the system's physical memory [70]. In a IoMT context, it

only applies to scenarios of small datasets or in systems with large storage capacity.

Figure 8 presents the algorithms with statistically similar outcomes. However, we are dealing with an unbalanced dataset, with seizure class being 20% of all instances in the dataset and non-seizure the additional 80%. In such circumstances, the accuracy alone misleads the model interpretation because the imbalanced dataset might bias the result. In this scenario, the Kappa normalizes the accuracy results and improve its understanding.

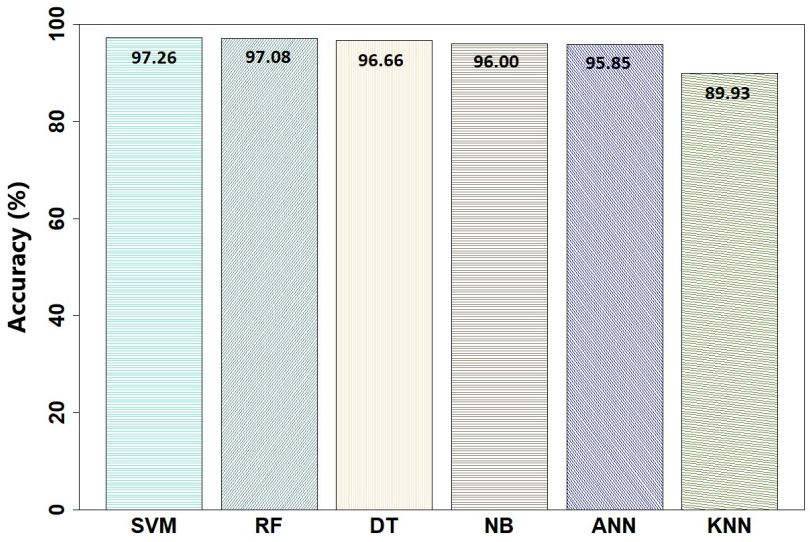

Figure 8: Accuracy for different ML algorithms in classifying epileptic seizures from EEG data.

The kappa results receive different interpretations depending on the analyst. The values presented in Table 7 for the strength of the kappa statistic are an arbitration accepted in the literature [71]. From the outcome of our experiments in Figure 9, five out of six classifiers presented results above 0.80, which is almost perfect. Additionally, SVM and RF outperformed DT, NB, and ANN with Kappa above 0.90. The KNN model resulted in Kappa between moderated and substantial, with a value of 0.6082. Thus, all investigated algorithms but KNN presented reliable and consistent results.

Table 7: Agreement measure for categorical data.

Kappa Statistic	Strength of Agreement
<0.00	Poor
0.00 - 0.20	Slight
0.21 - 0.40	Fair
0.41 - 0.60	Moderate
0.61 - 0.80	Substantial
0.81 - 1.00	Almost Perfect

Reciprocally, sensitivity provides the algorithm's capacity to avoid false negatives. In this indicator, the KNN model achieved the best result as an exhibit in Figure

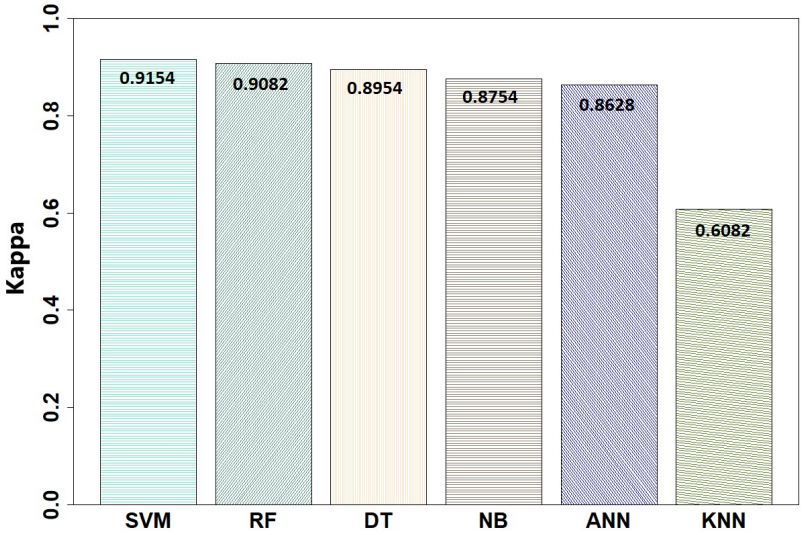

Figure 9: Kappa for different ML algorithms in classifying epileptic seizures from EEG data.

10. However, this is a direct effect of the binary classification on imbalanced data. The specificity results presented in Figure 11 confirms this analysis. The KNN model performed worse in isolating the false positives compared to the other five algorithms. The SVM and RF presented lower sensitivity; however, they exhibited higher specificity than the five tested ML alternatives. The Specificity results reinforce that SVM and RF have a high capacity to minimize false alarms. Putting the results together, *i.e.*, Accuracy, Kappa, and Specificity, in Table 8, we conclude that SVM and RF still present the best results compared with DT, NB, ANN, and KNN.

In an IoMT architecture, wearable devices provide physiological sensing. For clinical diagnostic, the IoMT devices can perform in-device or fog processing using ML algorithms. Thus, IoMT application for epileptic seizure detection requires availability, reliability, low latency, and fast response times. This scenario expects an algorithm with high Accuracy, Kappa, and Specificity combined with low computational complexity. As discussed in Chapter 3, many research works investigate epileptic seizure detection based on EEG analysis. On average, the surveyed articles achieve 94.31% of accuracy. Therefore, we define 94% as the baseline for the accuracy of any ML model applied for epileptic seizure detection. Concerning computational complexity, an algorithm executing in constant time, *i.e.*, *O(1)*, delivers the best solution [72]. Algorithms with *O(log n)* and *O(n)* complexity, with n equals to the dimensional of the dataset, performs worse than *O(1)* but still are good solutions. However, algorithms with computational complexity higher than *O(n log n)* are considered computationally expensive solutions. Thus, we assumed that an ML algorithm with complexity equal or better than *o(n log n)* potentially fits in an IoMT architecture to execute in-device or fog.

Table 8 summarizes the results achieved in this work. We present the Accu-

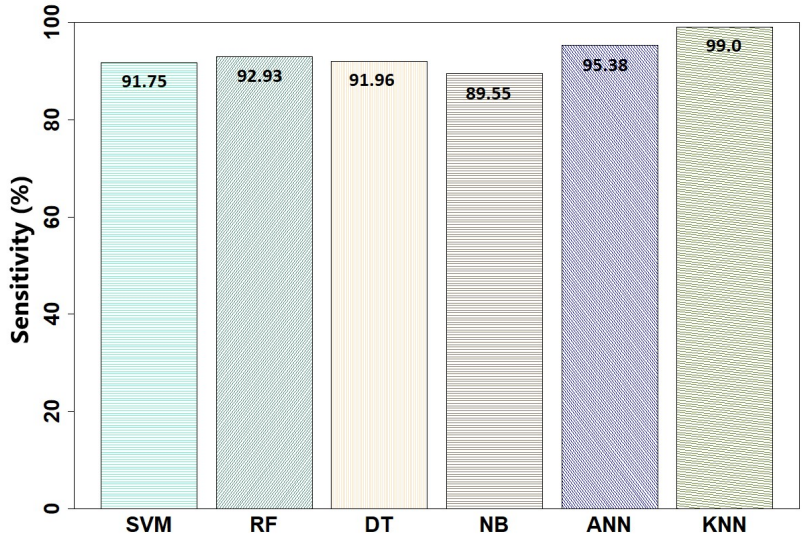

Figure 10: Sensitivity for different ML algorithms in classifying epileptic seizures from EEG data.

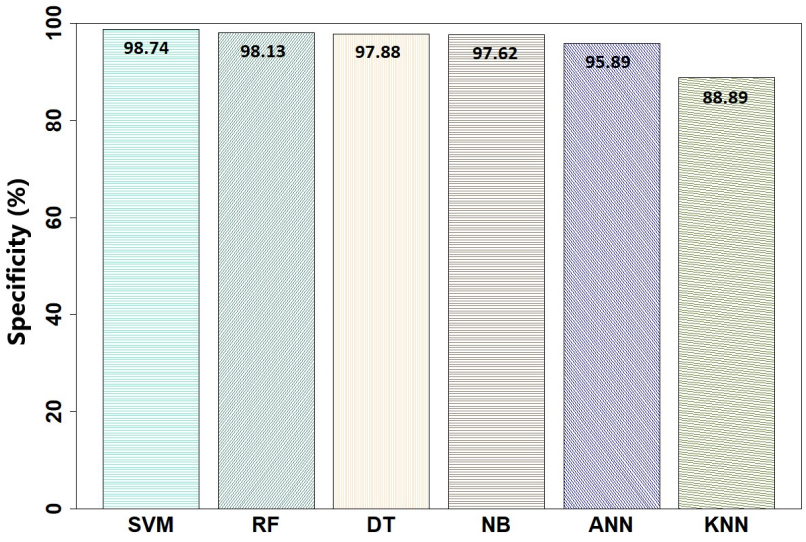

Figure 11: Specificity for different ML algorithms in classifying epileptic seizures from EEG data.

racy, Kappa, Specificity, and computational complexity, for the applicability in an IoMT context. The analysis considers A (for Applicable) or N/A (for Not Applicable). In this sense, SVM and RF present comparable outcomes. However, RF has lower computational complexity confronted with SVM. Hence, low computational complexity is an advantage in scenarios when the design requires continuous training to enhance accuracy. Thus, RF is a better choice for applications in an IoMT context.

Table 8: Performance results and complexity for the tested models

Algorithm	Accuracy (%)	Kappa	Specificity (%)	Computational Complexity	Applicability in Wearable
SVM	97.26	0.9154	98.74	$O(n^3)$	N/A
RF	97.08	0.9082	98.13	$O(n \log n)$	A
DT	96.66	0.8954	97.88	$O(\log n)$	NA
NB	96.00	0.8754	97.62	$O(m\ n)$	N/A
ANN	95.85	0.8628	95.89	$O(n^2)$	N/A
KNN	89.93	0.6082	88.89	space $O(n)$	N/A

4.5.1 The Ensemble Classifier Results

In this research, we analyze the stand-alone classifiers of different types. According to Witten and Frank [67], combining the individual's algorithms in an ensemble model likely enhances the overall system performance. Each stand-alone algorithm might perform better for specific features, and the ensemble capture whats is best from each of them. However, the ensemble model has two constraints: *(i)* the ML models originating it can not be strongly correlated, and *(ii)* the ML models can not perform poorly. If so, the stand-alone models will not carry too much information for the ensemble.

In Subsection 4.3.7 we explain three adopted strategies to combine the stand-alone models into on ensemble classifiers. Given that we analyze classifiers with heterogeneous concepts, the Stacking strategy is the right choice to combine our stand-alone results. Our implementation follows the strategy explained in Witten and Frank [73]. In this sense, the input for the ensemble model is the predictions of the stand-alone models. Moreover, the ensemble can be simplified using a tree or linear model, since the stand-alone models did all the heuristics [67]. Furthermore, in previous analysis we conclude that RF constitutes a good approach for application in the IoMT context. Hence, we implement the ensemble classifier using RF to combine the stand-alone models in pairs and triples.

The results in Table 9 presents the Accuracy and Kappa for the Ensemble model from the highest to the lowest accuracy. To obtain these results, we initially enrich the testing dataset with the predictions from the stand-alone models. Then, we train the Ensemble model using the RF algorithm against the enriched dataset. Finally, we validate the Ensemble model using the validation set. As illustrated in Table 9, combining SVM and ANN achieve 97.76%, roughly 0.5% better than SVM and 1.9% better than ANN stand-alone. Additionally, we verify an improvement in Kappa results due to the ensemble model.

Table 9: Accuracy and Kappa for Ensembled Models

Ensemble Model	Accuracy (%)	Kappa
SVM and ANN	97.76	0.9315
SVM and NB	97.70	0.9301
SVM and RF	97.63	0.9277
SVM, NB and KNN	97.07	0.9080
NB, KNN and ANN	96.97	0.9047
SVM, NB and ANN	96.92	0.9029

4.6 Final Remarks

The IoMT architecture composed of body sensors, communication gateway, and the central server is subject to several inaccuracy sources. According to Gravina *et al.* [74], motion artifacts, sensor's precision, sensor's calibration, and the limited sensor contact with body parts causes measurements to fail. In practical applications, an alternative to minimize the sensor's inaccuracy is to combine the information from different sensors. Thus, some authors dedicate their investigation to multi-sensor strategies and sensor fusion proposals [74, 60, 27].

In this research work, we analyze the ML algorithm in a stand-alone mode and configuring an ensemble. The aforementioned imprecision may decrease the ML accuracy and increase the false alarms. Thus, ML algorithms might perform worse in practical applications when compared with theoretical models. Hence, the application of an ensemble classifier enhanced the system performance in both accuracy and kappa Key Performance Indicators (KPI). Table 10 shows that our model presents promising results. The RF implementing the ensemble model has *O(n lg n)* complexity for training and retrieving data in the trees. Our model performs above average when compared with other related works and is better than models using ECG.

The application of an ensemble model opens the possibility for fusing different physiological information with one sole diagnostic purpose. Following the work from Mporas *et al.* [60] and Qaraqe *et al.* [27] on sensor fusion, RF could combine the different physiological information to detect epileptic seizures. Based on this lead, future research direction points for the combination of EEG and ECG. The EEG signal offers better features for epileptic seizure detection [26]. The ECG signal can provide both epileptic seizure detection [52, 53] and proof of life (user's authentication) [75, 76]. Thus, our proposal can evolve to a decision-making procedure considering two physiological data for seizure detection and one physiological information for identifying people with epilepsy.

Table 10: Our results compared with other authors

Author	Dataset	Algorithms	Complexity	Accuracy (%)	AuC
Polat and Günes [48]	EEG [37]	Welch FFT PCA AIRS with Fuzzy	$O(n\ log\ n)$ $O(min[p^3, n^3])$ $O(2^n)$	100.00	–
Polat and Günes [45]	EEG [37]	FFT DT	$O(n\ lg\ n)$ $O(lg\ k)$	98.72	–
Güler and Übeyli [42]	EEG [37]	WT ANFIS	$O(n)$ $O(2^n)$	98.68	–
THIS WORK	EEG [37]	Ensemble Model (using RF)	$O(n\ lg\ n)$	97.76	
Güler *et al.* [38]	EEG [37]	RNN with LE	$O(n^3)$	96.79	–
Hosseini *et al.* [50]	EEG [50]	WT I-ICA SVM	$O(n)$ $O(kn)$ $O(n^3)$	96.00	–
De Cooman *et al.* [52]	ECG [52]	HRI Extract SVM	$O(n)$ $O(n^3)$	81.89	–
Vandercasteele *et al.* [53]	ECG [53]	HRI Extract SVM	$O(n)$ $O(n^3)$	70.00	–
Neto *et al.* [20]	EEG	Classification Committee	–	–	0.7486

CHAPTER 5

Data Traffic Classification to Priority Access for Wireless Healthcare Application

In the third research question, we seek to answer how to provide better QoS to transmit the diagnostic information to the hospital server in an IoMT application scenario. In the best-case situation, the IoMT application expects a dedicated high-speed channel. However, the sensing devices typically connect to a gateway using a short-range and low-speed wireless technology [4, 10]. Once in the gateway, the IoMT application will compete for medium access in the network system to transmit the information to a central server.

In this Chapter, we present MAESTRO - a device management system to coordinate IoMT device transmission to the application server. The system architecture consists of two modules. In the first module, the **Classifier** identifies the physiological stream and assigns a required transmission priority according to a pre-defined QoS. In the second module, the **Prioritization** allocates the physiological flow to an appropriate network access category in the WiFi MAC layer according to the assigned priority. Our strategy has the advantage of enhancing transmission QoS for IoMT devices, depending on the therapy's medical requirements.

The remaining of this Chapter discusses the application scenario in Section 5.1. Section 5.2 explores the classification module in MAESTRO, describing the ML process, and the chosen ML algorithm. Section 5.3 presents the medium access control method considered in MAESTRO. Section 5.4 defines the evaluation metrics and discuss the achieved results for both classification and prioritization modules. Finally, we present our final remarks in Section 5.5.

5.1 System Overview

To contextualize this experiment, we consider the environment of a Health Park defined as a public space to promote preventive medicine initiatives [77]. In this environment, monitored patients and community citizens share the park facilities, including a WiFi network. We assume that community members use the network access for transmitting data such as voice, video, and web navigation to the internet. Patients are individuals requiring continuous monitoring. In this context, the patients might wear multiple IoMT sensing devices. The sensing devices transmit the physiological information to a smartphone operating as a gateway. Afterward, the gateway sends the data via the existing network infrastructure to a cloud server. Moreover, IoMT applications have strict data packet delivery and traffic delay requirements to ensure accurate information for medical staff [21, 22].

According to the patient's condition, the physiological data from the IoMT device add insights with distinct relevance for the diagnostic point of view [21]. The medical staff might indicate the significance of the physiological data for the therapy. Thus, heartbeat rate and blood pressure might be of high priority for a patient with a cardio condition. Alternatively, respiratory rate and oxygen saturation might be relevant for patients with pulmonary disease. Hence, the algorithm proposed in MAESTRO considers this information from the medical staff for the transmission priority assignment.

For IoMT applications, it is essential to classify the different medical traffic data transmitted from sensing devices in a shared wireless infrastructure [21]. Thus, MAESTRO runs the classification and prioritization modules, as shown in Figure 12. Notably, physiological information collected in IoMT devices such as ECG, blood pressure, respiration, and CO2 has distinct morphologies and sample rates. Figure 13 [78] illustrates the differences of ECG, arterial blood pressure, pulmonary artery pressure, central venous pressure, respiration, and CO2 rate obtained in Physionet databank [78]. The classification module identifies the vital sign based on the stream morphology, using a machine learning semi-supervised model running in the IoMT gateway. Afterward, based on the medical requirements and the significance during patient monitoring, MAESTRO assigns a target class with the desired transmission priority, without disclosing the patient's identity. The prioritization module designates a different network access category in the MAC layer based on the target classes. Thus, the prioritization module balances the data traffic in the EDCA access categories in the WiFi network. Next, we detail the classification and prioritization modules.

5.2 Classification Module

The medical crew assisting a patient defines the therapy according to the patient's condition. During anamnesis, the physician decides which physiological information or medical examination is relevant to investigate the patient's health. The MAESTRO

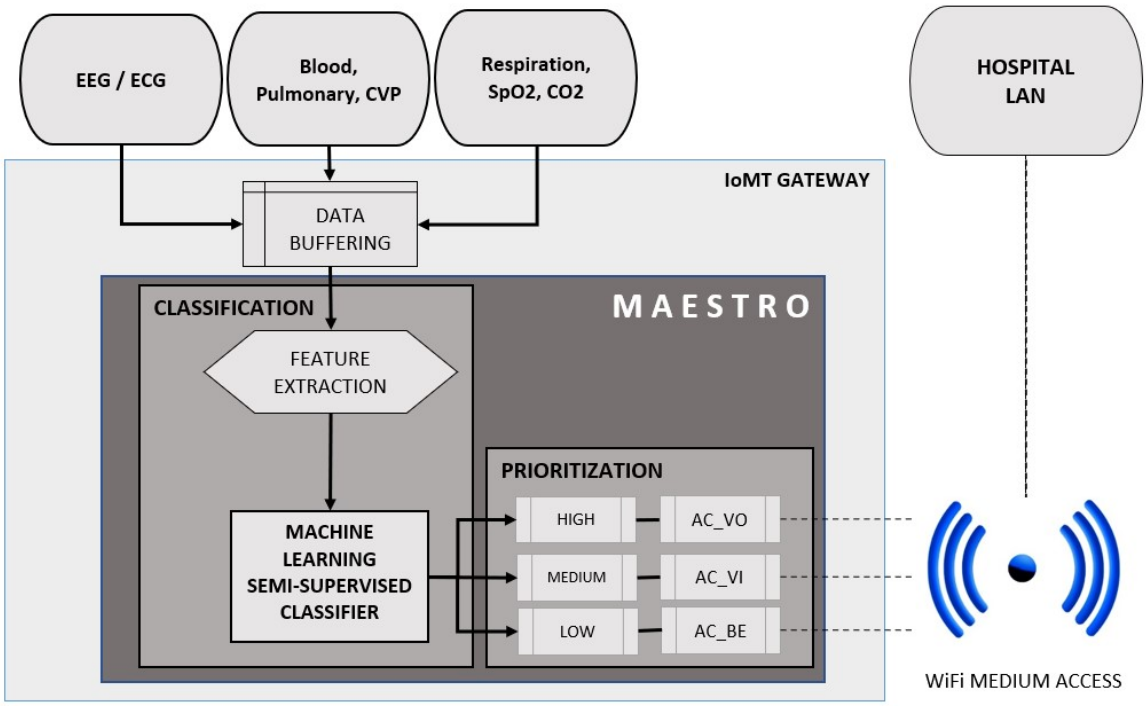

Figure 12: The MAESTRO System

Figure 13: Morphology of physiological information

classification module uses the same concept. In this sense, the medical crew defines the importance of each physiological information for the diagnostic and therapy. The MAESTRO system uses this information to label a physiological stream with the required transmission priority. The correct evaluation of the dataset is essential for the model's final result. Initial data inspection allows patterns and trends detection with descriptive statistics, visualization, and many other techniques. The results from the data analysis help to define the features that add more information for the problem resolution.

For the rest of this analysis, our work considers the dataset provided by the The Massachusetts General Hospital-Marquette Foundation (MGH-MF) on the Physionet Databank [78]. This dataset counts for 250 recordings of 3-lead ECG, Arterial Blood Pressure (ABP), Pulmonary Artery Pressure (PAP), Central Venous Pressure (CVP), respiration, and airway CO2 signals from patients in critical care units. After visual inspection, we identify anomalies in physiological data such as:

i) patients diverge in terms of the sensor data, *i.e.*, the dataset does not present the same physiological information for all patients.

ii) missing sensor data, *i.e.*, some of the physiological datasets present measurement errors after some time.

iii) sensors calibration and motion artifacts caused high noise levels in the initial and final segments of some streams.

Initially, this work assumes that MAESTRO will classify a balanced dataset. In this sense, we consider only patients with complete physiological data to address the anomaly *i*. Following, we solve anomalies *(ii)* and *(iii)* framing the physiological information with epochs of 1-second duration, eliminating the segments with abnormalities. To increase the dataset dimension, we concatenate the consecutive periods without overlapping, as illustrated in Figure 13 red frames. In this way, this work extracts the morphological waveforms from the physiological data to preserve the raw data for transmission. In this context, we buffer one second of physiological data from the IoMT sensing device, perform the feature selection, classify the information, assign the required priority in the data segment, and push the information to the prioritization module. Hence, the classification module does not insert a long processing delay before data transmission.

The literature refers to the ML process as supervised, unsupervised, or semi-supervised learning. On the one hand, supervised learning relates to classification and regression, requiring a set of labeled data to train the algorithms. A target class in the dataset contains the label that can be either categorical for classification or numerical for regression. On the other hand, unsupervised learning refers to clustering over a not-labeled dataset. Typically, the ML model creates clusters of similar information in the dataset. Finally, semi-supervised lies in between the latest two and consists of applying labels to a small dataset, training a model, and using the resultant model to tag a broader set. Hence, this work labeled a small dataset with the required priority and used a semi-supervised ML model to identify and assign priorities to a larger dataset. Applying the semi-supervised modeling adapts MAESTRO to classify the physiological data with different preferences for each patient.

Pawar and Mohammad [22] review the QoS metrics for data transmission in the context of a mobile patient's monitoring. The authors compile the requirements in terms of data rate, maximum delay, and maximum bit error rate based on the physiological sensor. Additionally, the authors define how critical is each physiological information according to the amount of data generated by the sensor. For the modeling of MAESTRO, our work

considered the significance of the physiological data derived from Pawar and Mohammad [22] as an exhibit in Table 11. The significance determined the required transmission priority.

Table 11: Importance assignment of physiological signs

	SIGNIFICANCE	
SENSOR	[22]	This Research
ECG	Medium	High
EEG	High	High
Blood Pressure	Low	Medium
Respiration	Low	Low
SpO2	Low	-
Accelerometer	Low	-
Sound Diagnostic	Medium	-
Medical Imaging (uncompressed)	Medium	-
Medical Imaging (ROI JPEG)	Medium	-
Video	Medium	-
CO2	-	Low
Pulmonary Pressure	-	Medium
Central Venous Pressure	-	Medium

We evaluate the classification module using algorithms based on probabilistic, tree, and distance methods. After considering Accuracy and Kappa as criteria, the classification function embedded in MAESTRO implements an NB probabilistic algorithm to classify the incoming traffic from IoMT devices and assign a required transmission priority. We propose the NB algorithm since it presented higher Accuracy and Kappa when compared with DT and KNN. As explained in Chapter 4, the NB algorithm derives from the conditional probability theory [64], where NB associates the probability of an event B to occur based on previous knowledge of an event A, as shown in Eq. 4.5.

5.3 Prioritization Module

In our research, the MAESTRO classification module classifies and labels the physiological data flows received from the IoMT devices. The labels reflect the significance of this vital sign data for the diagnostic. Hence, critical physiological information for the diagnostic requires higher transmission priority in the wireless network. Thus, we propose an adaptive medium access scheme to prioritize data transmission from IoMT devices to the cloud servers.

In the latest IEEE 802.11 amendment, the most adopted QoS strategy is EDCA. Notably, the EDCA parameters define four queues to control the medium access in the wireless channel: AC_BK, AC_BE, AC_VI, and AC_VO, respectively, background, best effort, video, and voice. According to the amendment, the access point shall announce the EDCA parameters [36]. When the transmitting station is a sensor device, each AC

queue assumes the settings expressed in Table 12 for CW, AIFSN, and TXOP. The MAESTRO prioritization module uses the tag assigned in the classification module to match the required access category to grant better QoS for IoMT devices following the algorithm 1. The ML module assigns the required priority in the first field of the stream. Hence, the prioritization module retrieves this information and push the data stream to a corresponding EDCA queue. For high priority medical data, the prioritization module drives the flow in the AC_VO queue. For medium priority, the flow goes to the AC_VI queue.

Algorithm 1 MAESTRO - prioritization module

Require: Incoming traffic
Ensure: prioritization by traffic type

```
1: procedure IoMTcheck
2:     if IncoTraf then                                   ▷ Incame IoMT traffic
3:         dataStream ← machineLearning(IncoTraf)         ▷ Predicts traffic type and assign
   QoS to dataStream
4:         myPriority ← dataStream[0]                     ▷ Read Priority Requirement
5:         if myPriority then
6:             switch[myPriority]                         ▷ Assign AC and user priority
7:                 case 1: dataStream.AC:= AC_VO; tid:=7; break;
8:
9:                 case 2: dataStream.AC:= AC_VI; tid:=5; break;
10:
11:                case 3: dataStream.AC:= AC_BE; tid:=3; break;
12:
13:            swEnd
14:        else                                           ▷ Reduces priority of other traffic types
15:            switch[AC]
16:                case AC_VO: tid:=6; break;
17:
18:                case AC_VI: tid:=4; break;
19:
20:                case AC_BE: tid:=3; break;
21:
22:            swEnd
```

Table 12: Set of EDCA parameters, if STA is a sensor device

AC	CWmin	CWmax	AIFSN	TXOP limit	Priority	MASTRO Queues
AC_BK	aCWmin	aCWmax	7	0	1 or 2	—
AC_BE	aCWmin	aCWmax	2	0	0 or 3	Low
AC_VI	(aCWmin+1)/2-1	aCWmin	5	0	4 or 5	Medium
AC_VO	(aCWmin+1)/4-1	(aCWmin+1)/2-1	4	0	6 or 7	High

In this work, we expand the concept explored in Vergutz *et al.* [17], concerning the AIFSN and CW parameters to transmit IoMT data. Also, we advance the strategy described in Kim *et al.* [12] on delaying background traffic to improve QoS for IoMT applications. Finally, we explore the conclusion from Patel and Choudhary [56], on balancing the traffic between three queues. Our approach does not depend on the congestion

level in the network. However, the simulation admits that the background traffic from internet station devices compromises 50% of the WiFi access point capacity.

5.4 Evaluation

To evaluate the MAESTRO effectiveness, we need to review the traffic classification and the prioritization modules individually. We implement the classification module in the R language, whereas we assess the network performance for prioritization through simulations in NS-3. As described in Chapter 4, the literature refers to precision-recall and accuracy-kappa, among others, as evaluation criteria for ML algorithms. The evaluations of the prioritization module considered the packet delivery ratio and network delay metrics as reference. Next, we detail the MAESTRO's implementation and evaluation.

5.4.1 Classification Module

The IoMT systems prefer sensors that measure vital signs, such as sensing of heartbeat, respiratory rates, pulse, blood pressure, and blood oxygen, crucial to determining the patient's health condition. Baker *et al.* [31] recommend to transfer raw data to the cloud servers. This recommendation suggests preserving as much information as possible for medical diagnostic. In this way, we consider the transmission of epochs with a one-second duration of raw physiological data.

For testing the MAESTRO system, we consider the MGH-MF dataset from the Physionet Databank [78], which contains physiological data from 250 patients monitored at the Massachusetts General Hospital. To address the issue listed in Section 5.2, we selected one hour of sensing data collected from 39 patients who displayed eight physiological measurements. We analyzed physiological data from patients with complete datasets for ECG (in three channels), arterial, pulmonary, central venous pressures, O2, and CO2 saturation.

To generate the data frame for classification, we proceed as follows. Initially, we define an observation window with one second of duration. This observation window buffers the physiological stream to select the segments for analysis. Then, we eliminated the anomalies associated with the sensor's calibration and motion artifacts in the initial and final sections of the physiological streams by advancing the observation window. Thus, the segments selected for analysis comes from the middle of the physiological data collection, when the signal is more stabilized. Following, we concatenate ten epochs of one-second duration from each physiological measurement. We repeat the process ten times to increase the data frame dimensions. According to this procedure, we provided a clean data frame for the ML model with 3120 examples of physiological data with ten seconds for each instance.

We follow the ML implementation available in the caret package in the R language version 3.5.1. In this implementation, we assess the Accuracy and Kappa for **NB**, **DT**,

and **KNN**, respectively, a probabilistic, a tree, and a distance-based algorithm. This assessment proposes identifying the best approach to recognize the physiological stream. To train and test the ML algorithms, we split the dataset into three equally distributed subsets. We train the algorithms using one-third of the dataset in a cross-validation 20-fold strategy. Next, we test the model's generalization capabilities using the second-third subset.

The classification module uses a semi-supervised process. First, we inspect and assigned the required transmission prioritization for each physiological example in the data frame. We consider the tuples sensor versus the prioritization expressed in Table 11. Hence, we established the priorities as HIGH, MEDIUM, and LOW according to our previous knowledge from the physiological data. For this experiment, we consider ECG and EEG high priority streams; the pressure measurements such as blood and pulmonary pressures are medium priority streams; respiration and CO2 receive low priority.

Figures 14 and 15 show the accuracy and kappa results for the three evaluated classifiers. All three evaluated ML algorithms achieved accuracy above 70%, but the probabilistic model, *i.e.*, the **NB** adapted better, achieving 91.5% accuracy. However, as explained in Chapter 4, the accuracy requires complementary information to conclude the analysis. In this sense, the kappa results show that only the NB algorithm performed above 0.8, which is considered almost perfect as an exhibit in Table 7. After evaluating the results in the train-test phase, we implement the **NB** algorithm in the MAESTRO classification module. Finally, we use the **NB** model to label the third subset, assigning the required priority, and transmitting the physiological data to the central server.

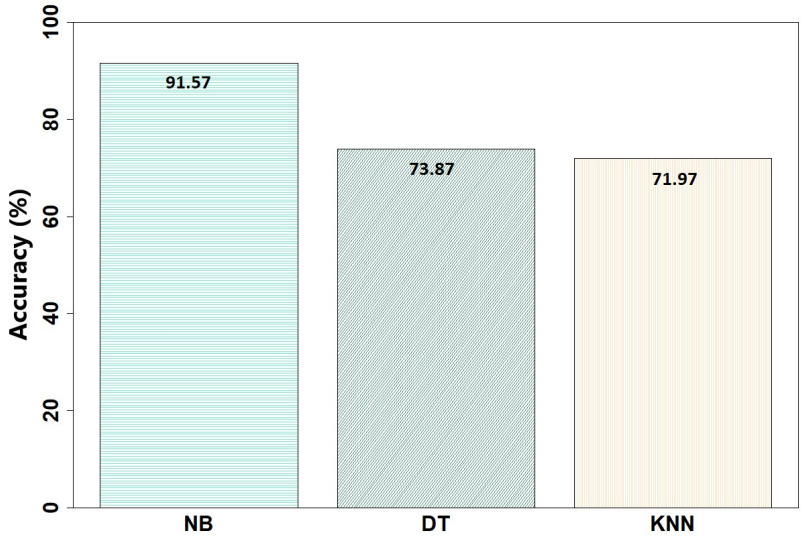

Figure 14: Accuracy in identifying the physiological streams

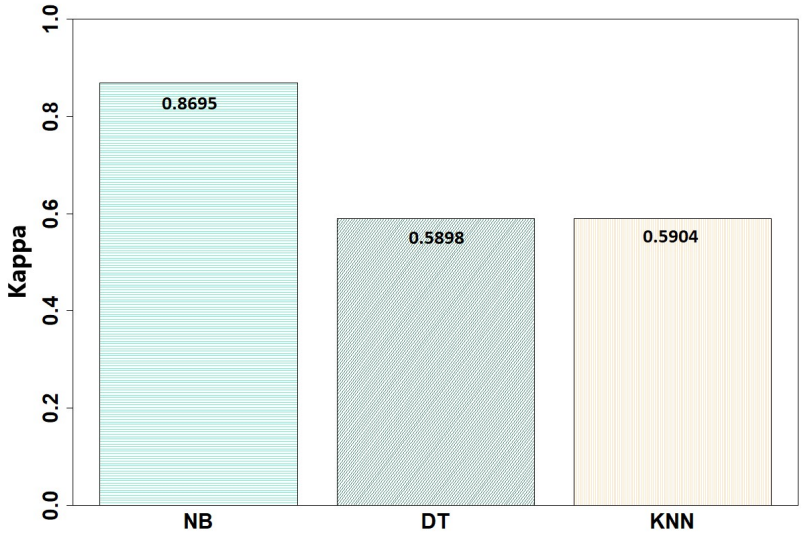

Figure 15: Kappa in identifying the physiological streams

5.4.2 Prioritization Module

For the network performance, we consider the PDR and network transmission delay as evaluation metrics. The PDR reflects the percentage of packets successfully transmitted from one node to another, in our simulation, from the gateway to the WiFi access point. The network transmission delay expresses the delay in milliseconds for a node to transmit a data packet and receives the respective acknowledgment from the receiving end. In our simulation scenario, the transmission delay considers only the air time in the wireless interface.

To evaluate our prioritization module, we simulated MAESTRO in NS-3. The simulator allows variations of topology and technologies, serving well for this investigation. To set up the simulation, we considered the IoMT devices surrounding the gateway forming a two-meter radius circle. We positioned the generic STA in a five-meter radius circle around the WiFi access point. The IoMT gateway and the WiFi access point are ten meters close to each other. Additionally, we placed the Hospital LAN node twenty-five meters away from the WiFi router.

Figure 16 exhibits the monitoring scenario. IoMT devices continuously collect patient's physiological information in Tier 1 and send data to the gateway in Tier 2. The gateway competes for medium access in the WiFi network with other generic STA to transmit the information to the hospital LAN server in Tier 3. We define the simulation scenario with five IoMT sensing devices per patient. We consider the number of monitored patients varying from 1 to 4. Thus, the number of IoMT devices ranges from 5 to 20 around the gateway. Simultaneously, we change the quantities of generic STA from 10 to 25. For each network configuration, we execute 30 rounds of simulations turning MAESTRO On and Off. We establish a background network traffic corresponding to 50% of the WiFi

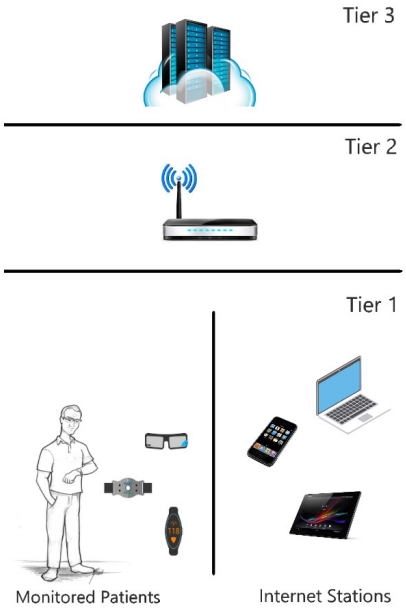

Figure 16: Three tier architecture for the prioritization module.

channel capacity, and three traffic profiles for the background, named *voice*, *video*, and *web navigation*. For generating competition for the medium in the WiFi network, we consider the three background traffic profiles adjusting to the AC_VO, AC_VI, and AC_BE in the EDCA queues. The AC_MD queue computes the traffic statistics from IoMT devices. In this context, we stressed the network behavior and captured the mean values for PDR and Delay.

Figure 17(a) shows the PDR under the network in a standard configuration, *i.e.*, without MAESTRO. The results without MAESTRO indicates that when the number of devices increases, the background traffic prevails over the IoMT traffic expressed in AC_MD. The EDCA QoS scheme grants more air time to Voice, Video, and web navigation, *i.e.*, AC_VO, AC_VI, AC_BE, respectively. When the network traffic increases, congestion causes packets to be dropped and lost. In an IoMT application scenario, there is a high risk that packet loss distorts the physiological information reaching the hospital server biasing the diagnostic procedures. In this scenario, the physiological data traffic competes in the best effort privileges. Thus, physiological data traffic exhibit in the curve of AC_MD receives a lower priority resulting in 35% lower PDR compared with Voice for 45 devices.

Figure 17(b) presents the PDR under the network considering MAESTRO. In our simulation, the prioritization module reduces the PDR for Voice, Video, and Internet traffic by 28%, 5%, and 5%, respectively. The results confirm that it is possible to increase the PDR in 60% for the IoMT device, as depicted in the AC_MD graphic. In this way, MAESTRO achieved higher efficiency since it modifies the EDCA parameters to grant more air time to IoMT data traffic. Effectively, MAESTRO reduces air time from the background traffic, *e.g.*, Voice, Video, and web navigation, distributes the physiological data traffic in three different queues, and finally sets the EDCA parameters equivalent to

AC_VO, AC_VI, and AC_BE for physiological data according to the required priority.

Figure 17(c) displays the PDR considering the traffic only for IoMT devices. In this scenario, the figure compares the traffic curve behavior considering or not the MAESTRO. These results complement the performance evidence, clearly showing the system's efficiency against a standard configuration, improving PDR for IoMT devices in 60%. The ML algorithm to classify physiological data packages, combined with the algorithm to assign the data flow to different network access categories in the MAC layer embedded in MAESTRO, grants the improvement.

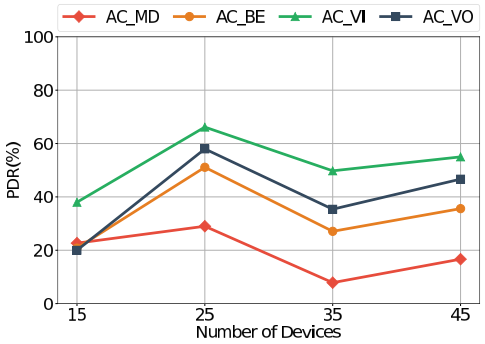

(a) All data traffic without MAESTRO

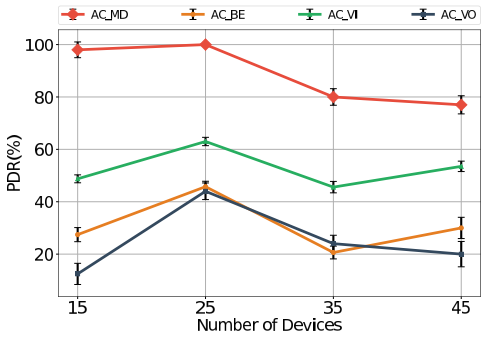

(b) All data traffic with MAESTRO

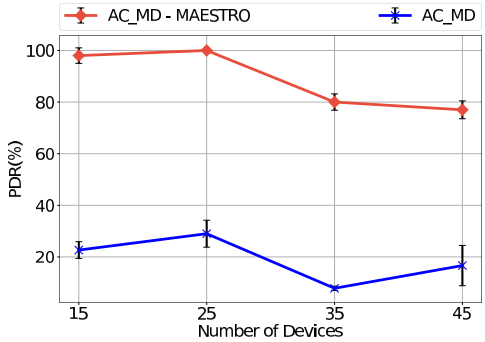

(c) Medical data with and without MAESTRO

Figure 17: PDR with and without MAESTRO considering different number of devices

Figure 18 shows the traffic delay only for IoMT devices, in the network scenario with and without MAESTRO. Analyzing the results, we conclude that MAESTRO reduced the traffic delay for IoMT devices compared to the transmission without MAESTRO. Accurately, the IoMT device's traffic transmitted without MAESTRO does not have any mechanism to prioritize this traffic compared to other generic traffic types. As discussed throughout this work, prioritization is fundamental since IoMT applications have strict requirements in terms of data delivery and delay to ensure accurate information for medical staff.

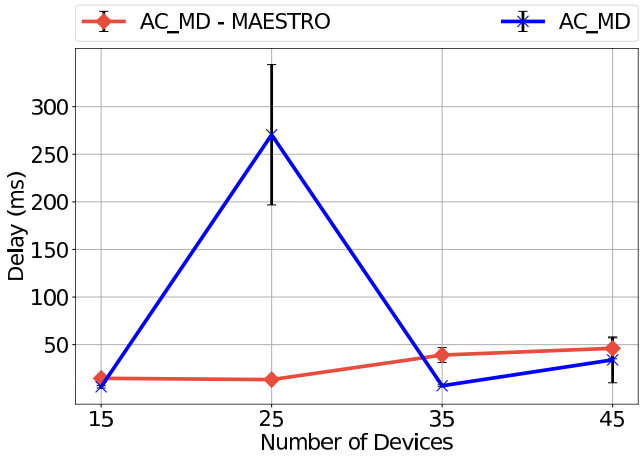

Figure 18: Delay for medical data with and without MAESTRO

5.5 Final Remarks

We present the MAESTRO system for medical device management to improve QoS for IoMT applications. MAESTRO applies a machine-learning algorithm to inspect the network data packets and identify the physiological information it holds. Additionally, the machine-learning module tags a priority to the physiological data. Next, a prioritization algorithm associates this priority with an equivalent access category in the WiFi network. Simulations determined that MAESTRO achieved 91.5% accuracy and 0.869 of Kappa in identifying and tagging the physiological data. The network simulations confirmed 60% of improvement in PDR compared to a standard transmission. Although presenting promising achievements for PDR, MAESTRO still requires improvement for the delay. As seen in Figure 18, there is an unexplained behavior in traffic delay when the network is serving 25 devices with MAESTRO. The prioritization scheme needs revision to address this issue, including scenarios with higher levels of network congestion.

CHAPTER 6

Conclusion

The increasing popularity of wearable devices such as smartwatches and wrist bands enhances the user's experience [4]. Wearable devices combined with mobile applications deliver solutions that a smartphone alone can not provide. These devices constitute the subjects of the IoT and thousands of IoT devices are already connected in the network [2]. The introduction of wearable devices for healthcare is a reality, with several state-of-the-art products available in the market, such as the Apple Watch 5, Samsung Galaxy Watch 3, and Xiaomi Mi Band 5. The IoMT associates IoT devices with healthcare applications. In this context, the introduction of ML methods to assist clinical diagnosis receives great attention from academy and industry [20, 27, 7, 15]

The IoMT applications are an alternative for monitoring patients with chronic conditions like epilepsy [15]. In this architecture, a wearable device continuously collects the user's physiological information, transfers the user data to a smartphone or gateway, and at the latest stage, the physiological information reaches a central server for processing. In this context, it is imperative to guarantee the proper QoS for such applications. For better efficiency, the IoMT applications require low latency and reliable network [2]. Additionally, continuous patient monitoring requires a broadband channel to transfer data to a central server.

In this work, we demonstrate that processing the clinical diagnostic near the patient, *e.g.*, in a smartphone acting as a gateway, improves the application QoS. An ML algorithm processing physiological data in the fog with low computational complexity provides the IoM solution with availability, reliability, and low latency required in such an application. Moreover, after diagnostic in the fog, it is equally essential that the physiological condition reach the medical crew in the hospital as fast as possible, with high PDR and minimum delay. This work proposes a potential solution to address this problem using ML.

6.1 Main Contributions and Thesis Summary

Our research considers that physiological data processing near the IoMT device, *i.e.*in the fog, minimizes the risk of compromising the data integrity, reducing the odds of missing something significant for the patient's therapy. Thus, fog processing requires transferring only the diagnostic data instead of all the physiological information. In this sense, we analyze the ML algorithms in the context of an IoMT application providing high accuracy in detecting epileptic seizures with low computational complexity. Moreover, we confirm that using an ensemble classifier enhances the ML model's efficiency. Based on the results, this research concludes that RF fulfills the required accuracy, the low computational complexity for an IoMT application, and fits well as an ensemble classifier to detect epileptic seizures.

Concerning data transmission, physiological information requires higher QoS levels to reach the medical crew with minimum delay. Our work develops the concepts for a transmission coordinator - the MAESTRO. In this proposal, the coordinator identifies the physiological traffic pattern originated in the IoMT device, assigns a tag associated with the required QoS, and provides higher transmission priority to the IoMT application. MAESTRO uses EDCA queues in the WiFi network to prioritize the physiological traffic, identifying the physiological stream with minimum delay.

Our main contribution is a framework that includes a clinical diagnostic for a chronic condition combined with traffic identification and prioritization. The concept is to assist medical crew outside hospital premises, allowing the patient's continuous monitoring. Moreover, our proposal is flexible, with both clinical diagnostic and traffic prioritization adaptable to an individual's medical condition. The epileptic seizure detection model requires only 10 seconds of EEG data to classify and detect a seizure. The traffic identification and prioritization module require only 1 second of physiological data to fulfill the classification.

6.2 Outlook

For the sequence of this research, we need to enhance the solution performance and link the ends. For the epileptic seizure detection, we will investigate other features in time-domain extracted from the EEG to provide higher information gain to the classification model. Additionally, we will develop a combination with the characteristics derived from the ECG. Specifically, the ECG provides characteristics allowing user's authentication and epileptic seizure detection. In this context, a combination of EEG and ECG for seizure detection and ECG for patient identification possibly enhances the system accuracy. Furthermore, the ensemble classifier is a potential solution to enhance accuracy combining ECG and EEG features. Finally, we will develop MAESTRO to process the end-to-end information in the following sequence:

1) receive the data streams

2) recognizes the characteristics of physiological information on the data stream.

3) use this information for clinical diagnostic, *i.e.*, epileptic seizure detection and user authentication

4) prioritize the transmission of the diagnostic information, even when the network is congested.

6.3 Published work

The main results obtained in this Ph.D. thesis were published in Resque *et al.* [15, 79] in the following events:

1. [15] - P. Resque, A. Barros, D. Rosário, and E. Cerqueira, "An investigation of different machine learning approaches for epileptic seizure detection," In Proceedings of the 15th International Wireless Communications & Mobile Computing Conference (IWCMC), Tangier, Morocco, 2019, pp. 301–306.
2. [79] - P. Resque, S. Pinheiro, D. Rosário, E. Cerqueira, A. Vergutz, M. Nogueira, and A. Santos, "Assessing data traffic classification to priority access for wireless healthcare application," In Proceedings of the IEEE Latin-American Conference on Communications (LATINCOM), Salvador, Brazil, 2019, pp. 1–6.

Complementary results were published in Santos *et al.* [80], Barros *et al.* [75], and Cerqueira *et al.* [81] in the following events:

1. [80] - A. Santos, I. Medeiros, P. Resque, D. Rosário, M. Nogueira, A. Santos, E. Cerqueira, and K. R. Chowdhury, "ECG-based user authentication and identification method on VANETs," in Proceedings of the 10th Latin America Networking Conference (LANC), São Paulo, Brazil, 2018, pp. 119–122
2. [75] - A. Barros, D. Rosário, P. Resque, and E. Cerqueira, "Heart of IoT: ECG as biometric sign for authentication and identification," In Proceedings of the 15th International Wireless Communications & Mobile Computing Conference (IWCMC), Tangier, Morocco, 2019, pp. 307–312.
3. [81] - E. Cerqueira, P. Resque, I. Medeiros, L. Bastos, A. Santos, T. Tavares, D. Rosário, A. Santos, and M. Nogueira, "Autenticação usando sinais biométricos: Fundamentos, aplicações e desafios." anais da Jornada de Atualização em Informática (JAI) do XXXIX Congresso da Sociedade Brasileira de Computação (CSBC 2019). SBC, June 2019, pp. 149–19
4. [76] - A. Barros, P. Resque, J. Almeida, R. Mota, H. Oliveira, D. Rosário, and E. Cerqueira, "Data Improvement Model Based on ECG Biometric for User Authentication and Identification". Sensors, vol. 20, no. 10, p. 2920, 2020.

References

[1] D. Koutras, G. Stergiopoulos, T. Dasaklis, P. Kotzanikolaou, D. Glynos, and C. Douligeris, "Security in iomt communications: A survey," *Sensors*, vol. 20, no. 17, p. 4828, 2020. Cited on page(s): 17

[2] Ericsson, "Mobility report," Available Online at https://www.ericsson.com/en/mobility-report/reports/november-2019, 2019. Cited on page(s): 17, 69

[3] R. Mota, A. Riker, and D. Rosário, "Adjusting group communication in dense internet of things networks with heterogeneous energy sources," in *Anais do XI Simposio Brasileiro de Computacao Ubiqua e Pervasiva*. SBC, 2019. Cited on page(s): 17

[4] S. Seneviratne, Y. Hu, T. Nguyen, G. Lan, S. Khalifa, K. Thilakarathna, M. Hassan, and A. Seneviratne, "A survey of wearable devices and challenges," *IEEE Communications Surveys & Tutorials*, 2017. Cited on page(s): 18, 40, 57, 69

[5] Z. Guan, Z. Lv, X. Du, L. Wu, and M. Guizani, "Achieving data utility-privacy tradeoff in internet of medical things: A machine learning approach," *Future Generation Computer Systems*, vol. 98, pp. 60 – 68, 2019. [Online]. Available: http://www.sciencedirect.com/science/article/pii/S0167739X18327195 Cited on page(s): 18, 19

[6] H. Habibzadeh, K. Dinesh, O. Rajabi Shishvan, A. Boggio-Dandry, G. Sharma, and T. Soyata, "A survey of healthcare internet of things (hiot): A clinical perspective," *IEEE Internet of Things Journal*, vol. 7, no. 1, pp. 53–71, Jan 2020. Cited on page(s): 18

[7] A. Mishra and M. Mohapatro, "An iot framework for bio-medical sensor data acquisition and machine learning for early detection," *International Journal of Advanced Technology and Engineering Exploration*, vol. 6, pp. 112–125, 06 2019. Cited on page(s): 18, 69

[8] F. Al-Turjman, M. H. Nawaz, and U. D. Ulusar, "Intelligence in the internet of medical things era: A systematic review of current and future trends," *Computer*

Communications, vol. 150, pp. 644 – 660, 2020. [Online]. Available: http://www.sciencedirect.com/science/article/pii/S0140366419313337 Cited on page(s): 18, 37

[9] N. Matni, J. Moraes, L. Pacheco, D. Rosário, H. Oliveira, E. Cerqueira, and A. V. Neto, "Experimenting Long Range Wide Area Network in an e-Health Environment: Discussion and Future Directions," in *proceedings of 15th International Wireless Communications & Mobile Computing Conference (IWCMC 2020)*. IEEE, November 2020. Cited on page(s): 18

[10] F. A. Kraemer, A. E. Braten, N. Tamkittikhun, and D. Palma, "Fog computing in healthcare - a review and discussion," *IEEE Access*, vol. 5, pp. 9206–9222, 2017. Cited on page(s): 18, 19, 33, 49, 57

[11] M. M. Alam, H. Malik, M. I. Khan, T. Pardy, A. Kuusik, and Y. Le Moullec, "A survey on the roles of communication technologies in iot-based personalized healthcare applications," *IEEE Access*, vol. 6, pp. 36 611–36 631, 2018. Cited on page(s): 18, 19, 23

[12] Y. Kim, S. Lee, and S. Lee, "Coexistence of zigbee-based wban and wifi for health telemonitoring systems," *IEEE journal of biomedical and health informatics*, vol. 20, no. 1, pp. 222–230, 2016. Cited on page(s): 19, 25, 36, 38, 62

[13] R. Ali, Y. A. Qadri, Y. B. Zikria, T. Umer, B.-S. Kim, and S. W. Kim, "Q-learning-enabled channel access in next-generation dense wireless networks for iot-based ehealth systems," *EURASIP Journal on Wireless Communications and Networking*, vol. 2019, no. 1, pp. 1–12, 2019. Cited on page(s): 19

[14] D. Rosário, M. Schimuneck, J. Camargo, J. Nobre, C. Both, J. Rochol, and M. Gerla, "Service Migration from Cloud to Multi-tier Fog Nodes for Multimedia Dissemination with QoE Support," *Sensors*, vol. 18, no. 2, 2018. Cited on page(s): 19

[15] P. Resque, A. Barros, D. Rosário, and E. Cerqueira, "An investigation of different machine learning approaches for epileptic seizure detection," in *2019 15th International Wireless Communications & Mobile Computing Conference (IWCMC)*. IEEE, 2019, pp. 301–306. Cited on page(s): 19, 69, 71

[16] A. H. Sodhro, Z. Luo, A. K. Sangaiah, and S. W. Baik, "Mobile edge computing based qos optimization in medical healthcare applications," *Intern. Journal of Information Management*, vol. 45, pp. 308–318, 2019. Cited on page(s): 19, 36, 38

[17] A. Vergütz, R. da Silva, J. A. M. Nacif, A. B. Vieira, and M. Nogueira, "Mapping critical illness early signs to priority alert transmission on wireless networks," in *Communications (LATINCOM), 2017 IEEE 9th Latin-American Conference on*. IEEE, 2017, pp. 1–6. Cited on page(s): 19, 34, 38, 62

[18] A. Tsinganos, Panagiotis; Skodras, "A smartphone-based fall detection system for the elderly," in *In Proceedings of the 10th International Symposium on Image and Signal Processing and Analysis*. IEEE, 2017. Cited on page(s): 19, 45

[19] A. Subasi, J. Kevric, and M. Abdullah Canbaz, "Epileptic seizure detection using hybrid machine learning methods," *Neural Computing and Applications*, Apr 2017. Cited on page(s): 19

[20] A. Neto, L. da Silva, R. Moioli, F. Brasil, and J. J. Rodrigues, "Predicting epileptic seizures: Case studies harnessing machine learning," in *ICC 2020-2020 IEEE International Conference on Communications (ICC)*. IEEE, 2020, pp. 1–6. Cited on page(s): 19, 32, 33, 47, 56, 69

[21] K.-J. Park, H.-H. Lee, S. Choi, and K. Kang, "Design of a medical-grade qos metric for wireless environments," *Transactions on Emerging Telecommunications Technologies*, vol. 27, no. 8, pp. 1022–1029, 2016. Cited on page(s): 19, 35, 58

[22] P. A. Pawar and S. P. Mohammad, "Review of quality of service in the mobile patient monitoring systems," in *IEEE Region 10 Symposium (TENSYMP), 2017*. IEEE, 2017, pp. 1–6. Cited on page(s): 19, 58, 60, 61

[23] M. M. Hassan, K. Lin, X. Yue, and J. Wan, "A multimedia healthcare data sharing approach through cloud-based body area network," *Future Generation Computer Systems*, vol. 66, pp. 48–58, 2017. Cited on page(s): 19, 33, 38

[24] World Health Organization, "Epilepsy," Available at http://www.who.int/mediacentre/factsheets/fs999/en/ (2017/11/17), 2017. Cited on page(s): 22, 43

[25] Brazil's Ministry of Health, "Clinical practices guidelines," Available at http://portalarquivos.saude.gov.br/campanhas/2014/Protocolos_clinicos/publication.pdf (2017/11/03), 2013. Cited on page(s): 22

[26] W. Tatum, G. Rubboli, P. Kaplan, S. Mirsatari, K. Radhakrishnan, D. Gloss, L. Caboclo, F. Drislane, M. Koutroumanidis, D. Schomer *et al.*, "Clinical utility of eeg in diagnosing and monitoring epilepsy in adults," *Clinical Neurophysiology*, vol. 129, no. 5, pp. 1056–1082, 2018. Cited on page(s): 22, 23, 39, 41, 55

[27] M. Qaraqe, M. Ismail, E. Serpedin, and H. Zulfi, "Epileptic seizure onset detection based on eeg and ecg data fusion," *Epilepsy & Behavior*, vol. 58, pp. 48–60, 2016. Cited on page(s): 22, 23, 55, 69

[28] V. Jurcak, D. Tsuzuki, and I. Dan, "10/20, 10/10, and 10/5 systems revisited: their validity as relative head-surface-based positioning systems," *Neuroimage*, vol. 34, no. 4, pp. 1600–1611, 2007. Cited on page(s): 22, 23

[29] J. Hundertmark, S. K. Apondo, and J.-H. Schultz, "Integrating teaching into routine outpatient care: the design and evaluation of an ambulatory training concept (heisa)," *GMS journal for medical education*, vol. 35, no. 1, 2018. Cited on page(s): 22

[30] Y. Chen, H. Li, L. Hou, and X. Bu, "Feature extraction using dominant frequency bands and time-frequency image analysis for chatter detection in milling," *Precision Engineering*, vol. 56, pp. 235 – 245, 2019. [Online]. Available: http://www.sciencedirect.com/science/article/pii/S0141635918304410 Cited on page(s): 23

[31] S. B. Baker, W. Xiang, and I. Atkinson, "Internet of things for smart healthcare: Technologies, challenges, and opportunities," *IEEE Access*, vol. 5, pp. 26 521–26 544, 2017. Cited on page(s): 23, 63

[32] A. Laya, C. Kalalas, F. Vazquez-Gallego, L. Alonso, and J. Alonso-Zarate, "Goodbye, aloha!" *IEEE access*, vol. 4, pp. 2029–2044, 2016. Cited on page(s): 25

[33] L. Leonardi, F. Battaglia, and L. L. Bello, "Rt-lora: A medium access strategy to support real-time flows over lora-based networks for industrial iot applications," *IEEE Internet of Things Journal*, 2019. Cited on page(s): 25

[34] A. Ahad, M. Tahir, and K. A. Yau, "5g-based smart healthcare network: Architecture, taxonomy, challenges and future research directions," *IEEE Access*, vol. 7, pp. 100 747–100 762, 2019. Cited on page(s): 25

[35] "Ieee standard for information technology—telecommunications and information exchange between systems local and metropolitan area networks—specific requirements - part 11: Wireless lan medium access control (mac) and physical layer (phy) specifications," *IEEE Std 802.11-2016 (Revision of IEEE Std 802.11-2012)*, pp. 1–3534, 2016. Cited on page(s): 25, 26

[36] IEEE, "Wireless lan medium access control (mac) and physical layer (phy) specifications. amendment 2: Sub 1 ghz license exempt operation," Available at https://ieeexplore.ieee.org/stamp/stamp.jsp?tp=&arnumber=7920364 (2018/12/19), 2016. Cited on page(s): 26, 61

[37] R. G. Andrzejak, F. Lehnertz, Klaus.and Mormann, C. Rieke, D. Peter., and C. E. Elger, "Indications of nonlinear deterministic and finite dimensional structures in time series of brain electrical activity: Dependence on recording region and brain state," *Phys. Rev. E 64, 061907*, 2001. Cited on page(s): 28, 29, 30, 33, 40, 43, 56

[38] N. F. Güler, E. D. Übeyli, and I. Güler, "Recurrent neural networks employing lyapunov exponents for eeg signals classification," *Expert systems with applications*, vol. 29, no. 3, pp. 506–514, 2005. Cited on page(s): 29, 33, 56

[39] G. Valenza, L. Citi, R. Barbieri, and R. Balasubramaniam, "Estimation of instantaneous complex dynamics through lyapunov exponents: A study on heartbeat dynamics," *PLoS ONE*, vol. 9, 2014. Cited on page(s): 29

[40] C. Yang and C. Q. Wu, "A robust method on estimation of lyapunov exponents from a noisy time series," *Nonlinear Dynamics*, vol. 64, pp. 279–292, 2011. Cited on page(s): 29

[41] J. Bilski, J. Smolag, and J. M. Żurada, *Parallel Approach to the Levenberg-Marquardt Learning Algorithm for Feedforward Neural Networks*. Springer International Publishing, 2015, pp. 3–14. Cited on page(s): 29, 50

[42] I. Güler and E. D. Übeyli, "Adaptive neuro-fuzzy inference system for classification of eeg signals using wavelet coefficients," *Journal of neuroscience methods*, vol. 148, no. 2, pp. 113–121, 2005. Cited on page(s): 29, 33, 56

[43] A. Muñoz, R. Ertlé, and M. Unser, "Continuous wavelet transform with arbitrary scales and o(n) complexity," *SIGNAL Processing*, vol. 82, pp. 749–757, 2002. Cited on page(s): 29

[44] R. K. Yadav and M. Balakrishnan, "Comparative evaluation of arima and anfis for modeling of wireless network traffic time series," *EURASIP Journal on Wireless Communication and Networking*, 2014. Cited on page(s): 30

[45] K. Polat and S. Güneş, "Classification of epileptiform eeg using a hybrid system based on decision tree classifier and fast fourier transform," *Applied Mathematics and Computation*, vol. 187, no. 2, pp. 1017–1026, 2007. Cited on page(s): 30, 33, 56

[46] S. Oraintara, Y.-J. Chen, and T. Q. Nguyen, "Integer fast fourier transform," *IEEE Transactions on Signal Processing*, vol. 50, no. 3, pp. 607–618, 2002. Cited on page(s): 30

[47] A. E. Choromanska and J. Langford, "Logarithmic time online multiclass prediction," in *Advances in Neural Information Processing Systems 28*, C. Cortes, N. D. Lawrence, D. D. Lee, M. Sugiyama, and R. Garnett, Eds. Curran Associates, Inc., 2015, pp. 55–63. Cited on page(s): 30, 50

[48] K. Polat and S. Güneş, "Artificial immune recognition system with fuzzy resource allocation mechanism classifier, principal component analysis and fft method based new hybrid automated identification system for classification of eeg signals," *Expert Systems with applications*, vol. 34, no. 3, pp. 2039–2048, 2008. Cited on page(s): 30, 33, 56

[49] I. M. Johnstone and A. Y. Lu, "Sparse principal components analysis," 2004, available at https://pdfs.semanticscholar.org/96bc/d3f00138d972a023ac9b00d038c47ad37ece.pdf (2017/12/03). Cited on page(s): 30

[50] M.-P. Hosseini, A. Hajisami, and D. Pompili, "Real-time epileptic seizure detection from eeg signals via random subspace ensemble learning," in *2016 IEEE international conference on autonomic computing (ICAC)*. IEEE, 2016, pp. 209–218. Cited on page(s): 30, 31, 33, 56

[51] A. Abdiansah and R. Wardoyo, "Time complexity analysis of support vector machines (svm) in libsvm," *International Journal of Computer Applications*, vol. 128, 2015. Cited on page(s): 31, 50

[52] T. De Cooman, C. Varon, B. Hunyadi, W. Van Paesschen, L. Lagae, and S. Van Huffel, "Online automated seizure detection in temporal lobe epilepsy patients using single-lead ecg," *International Journal of Neural Systems*, vol. 27, 2017. Cited on page(s): 31, 33, 55, 56

[53] K. Vandecasteele, T. De Cooman, Y. Gu, E. Cleeren, K. Claes, W. V. Van Paesschen, S. V. Huffel, and B. Hunyadi, "Automated epileptic seizure detection based on wearable ecg and ppg in a hospital environment," *Sensors*, vol. 17, no. 10, 2017. Cited on page(s): 31, 33, 55, 56

[54] P. P. M. Shanir, Y. U. Khan, and O. Farooq, "Time domain analysis of eeg for automatic seizure detection," in *In Proceedings of Emerging Trends in Electrical And Electronics Engineering*, 2015. Cited on page(s): 32

[55] N. Yessad, M. Omar, A. Tari, and A. Bouabdallah, "Qos-based routing in wireless body area networks: A survey and taxonomy," *Computing*, vol. 100, no. 3, pp. 245–275, 2018. Cited on page(s): 33, 34

[56] M. Patel and N. Choudhary, "A dynamic cross-layer mapping to support real time multimedia application over ieee 802.11n," in *2017 International Conference on Energy, Communication, Data Analytics and Soft Computing (ICECDS)*. IEEE, 2017, pp. 3474–3478. Cited on page(s): 35, 38, 62

[57] A. H. Sodhro, A. S. Malokani, G. H. Sodhro, M. Muzammal, and L. Zongwei, "An adaptive qos computation for medical data processing in intelligent healthcare applications," *Neural Computing and Applications*, pp. 1–12, 2019. Cited on page(s): 36, 38

[58] Y. Gu, E. Cleeren, J. Dan, K. Claes, W. Van Paesschen, S. Van Huffel, and B. Hunyadi, "Comparison between scalp eeg and behind-the-ear eeg for development of a wearable seizure detection system for patients with focal epilepsy," *Sensors*, vol. 18, no. 1, p. 29, 2018. Cited on page(s): 40

[59] M. Lichman, "Uci machine learning repository," 2013, available at https://archive.ics.uci.edu/ml/datasets/Epileptic+Seizure+Recognition (2020/03/01). Cited on page(s): 40, 41, 43

[60] I. Mporas, V. Tsirka, E. I. Zacharaki, M. Koutroumanidis, M. Richardson, and V. Megalooikonomou, "Seizure detection using eeg and ecg signals for computer-based monitoring, analysis and management of epileptic patients," *Expert systems with applications*, vol. 42, no. 6, pp. 3227–3233, 2015. Cited on page(s): 42, 55

[61] M. Yesilbudak, S. Sagiroglu, and I. Colak, "A novel implementation of knn classifier based on multi-tupled meteorological input data for wind power prediction," *Energy Conversion and Management*, vol. 13, pp. 434–444, 2017. Cited on page(s): 45

[62] D. K. Tayal, A. Jain, S. Arora, S. Agarwal, T. Gupta, and N. Tyagi, "Crime detection and criminal identification in India using data mining techniques," *AI and Society*, vol. 30, pp. 117–127, 2015. Cited on page(s): 45

[63] P. P. M. Shanir, K. A. Khan, Y. U. Khan, O. Farooq, and H. Adeli, "Automatic seizure detection based on morphological features using one-dimensional local binary pattern on long-term eeg," *Clinical EEG and Neuroscience*, 2017. Cited on page(s): 45

[64] I. Goodfellow, Y. Bengio, and A. Courville, *Deep Learning*. MIT Press, 2016, http://www.deeplearningbook.org. Cited on page(s): 45, 61

[65] S. Haykin, *Neural networks and learning machines*. Pearson Education Inc., 2008. Cited on page(s): 46

[66] F. Araújo, F. Araújo, K. Machado, D. Rosário, E. Cerqueira, and L. A. Villas, "Ensemble mobility predictor based on random forest and markovian property using lbsn data," *Journal of Internet Services and Applications*, vol. 11, no. 1, pp. 1–11, 2020. Cited on page(s): 47

[67] I. H. Witten. and E. Frank, *Data mining: Practical machine learning tools and techniques 2nd edition*, ser. Morgan Kaufmann series in data management systems. Elsevier, 2005. Cited on page(s): 47, 54

[68] M. Hossin and M. Sulaiman, "A review on evaluation metrics for data classification evaluations," *International Journal of Data Mining & Knowledge Management Process*, vol. 5, no. 2, p. 1, 2015. Cited on page(s): 48

[69] H. Ahmadi and R. Bouallegue, "Comparative study of learning-based localization algorithms for wireless sensor networks: Support vector regression, neural network and na amp;x00ef;ve bayes," in *2015 International Wireless Communications and Mobile Computing Conference (IWCMC)*, Aug 2015, pp. 1554–1558. Cited on page(s): 50

[70] A. Lodwich, F. Shafait, and T. M. Breuel, "Efficient estimation of k for the nearest neighbors class of methods," *CoRR*, vol. abs/1606.02617, 2016. Cited on page(s): 50

[71] A. J. Viera, J. M. Garrett *et al.*, "Understanding interobserver agreement: the kappa statistic," *Fam med*, vol. 37, no. 5, pp. 360–363, 2005. Cited on page(s): 51

[72] T. H. Cormen., C. E. Leiserson., R. L. Rivest., and C. Stein, *Introduction to Algorithms*. MIT Press, 2009. Cited on page(s): 52

[73] F. Azuaje, "Witten ih, frank e: Data mining: Practical machine learning tools and techniques 2nd edition," 2006. Cited on page(s): 54

[74] R. Gravina, P. Alinia, H. Ghasemzadeh, and G. Fortino, "Multi-sensor fusion in body sensor networks: State-of-the-art and research challenges," *Information Fusion*, vol. 35, pp. 68–80, 2017. Cited on page(s): 55

[75] A. Barros, D. Rosário, P. Resque, and E. Cerqueira, "Heart of iot: Ecg as biometric sign for authentication and identification," in *proceedings of the 15th International Wireless Communications & Mobile Computing Conference (IWCMC)*. IEEE, 2019, pp. 307–312. Cited on page(s): 55, 71

[76] A. Barros, P. Resque, J. Almeida, R. Mota, H. Oliveira, D. Rosário, and E. Cerqueira, "Data improvement model based on ecg biometric for user authentication and identification," *Sensors*, vol. 20, no. 10, p. 2920, 2020. Cited on page(s): 55, 71

[77] R. Arena, S. Bond, R. O'Neil, D. R. Laddu, A. P. Hills, C. J. Lavie, and A. McNeil, "Public park spaces as a platform to promote healthy living: Introducing a healthpark concept," *Progress in Cardiovascular Diseases*, 5 2017. Cited on page(s): 58

[78] J. P. Welch, P. J. Ford, R. S. Teplick, and R. M. Rubsamen, "The massachusetts general hospital-marquette foundation hemodynamic and electrocardiographic database – comprehensive collection of critical care waveforms," Available at https://physionet.org/physiobank/database/mghdb/ (2018/12/19), 1991. Cited on page(s): 58, 60, 63

[79] P. Resque, S. Pinheiro, D. Rosário, E. Cerqueira, A. Vergutz, M. Nogueira, and A. Santos, "Assessing data traffic classification to priority access for wireless healthcare application," in *2019 IEEE Latin-American Conference on Communications (LATINCOM)*, 2019, pp. 1–6. Cited on page(s): 71

[80] A. Santos, I. Medeiros, P. Resque, D. Rosário, M. Nogueira, A. Santos, E. Cerqueira, and K. R. Chowdhury, "Ecg-based user authentication and identification method on vanets," in *Proceedings of the 10th Latin America Networking Conference*, ser.

LANC '18. New York, NY, USA: Association for Computing Machinery, 2018, p. 119–122. [Online]. Available: https://doi.org/10.1145/3277103.3277138 Cited on page(s): 71

[81] E. Cerqueira, P. Resque, I. Medeiros, L. Bastos, A. Santos, T. Tavares, D. Rosário, A. Santos, and M. Nogueira, "Autenticação usando sinais biométricos: Fundamentos, aplicações e desafios." in *38 Jornada de Atualização em Informática (JAI) do XXXIX Congresso da Sociedade Brasileira de Computação (CSBC 2019)*. SBC, June 2019, pp. 149–195. [Online]. Available: http://dx.doi.org/10.5753/sbc.471.7.04 Cited on page(s): 71